CHARACTERISATION OF THICK LIQUIDS USING A VIBRATING TRANSDUCER

PREPARED BY O.S Mlambo

PREPARED FOR Department of Electrical and Electronic Engineering at the University of Cape Town

SUPERVISED BY Professor J. Bell

September 2000

Thesis in full fulfilment of the requirements for an MSc degree in Electrical and Electronic Engineering.

ACKNOWLEDGEMENTS

Firstly I would like to thank God for always been on my side and the following people for all the support and assistance they have given me.

To my supervisor Prof Bell, for his willingness, availability and directions in all phases of this thesis.

To Jevon for sharing his ideas and experience on the subject. To Craig for always letting me print from his computer. To Joseph Dlamini, Larry Khuvutlu and Tebogo for helping me with the typing.

To my family especially my mother for always been on my side when times were tough. To Resego and Ofentse for always motivating me.

Lastly but never least, my girlfriend "Lolo" and my friends for their support.

SYNOPSIS

This report describes in detail all the work carried out to reach the main objective of this thesis project, which is to develop a tuning fork into a portable instrument used for the characterisation of thick liquids based on their density and viscosity.

A number of tuning forks were built and used in the development stages. They were driven magnetostrictively through their drive coils and set to resonance using a controllable amplified burst signal from the drive circuit.

On the listen mode the coil of the fork was connected to the listen circuit by a "Gunther" relay switch. So, when the fork rapidly recovered from the drive, its mechanical vibrations changed to electrical signals, which when amplified could be seen on the oscilloscope. The signals observed on the digital and analogue oscilloscopes could be captured in the computer for later analyses if required.

When a fork is driven in liquids its resonant frequency decreases due to the mass loading exerted by the liquid, hence a fork could be used to measure the liquid's density. The thickness of the liquid under examination also heavily loads a vibrating fork, leading to a very low Q factor. The inverse of Q is the loss angle and it gives a measure of the viscosity of the liquid tested or simply its thickness.

Tuning forks with different sensitivities were used in a range of liquids including paraffin, water, engine oil and glycerol. The frequency and the Q measurements were recorded and analysed each time. It was generally found that the frequency drops more in glycerol, water, engine oil and lastly paraffin. The measurements for the Q values obtained were on the other hand very high in paraffin followed by water, engine oil and glycerol respectively.

Finally the main objective of the project was achieved, where an instrument for general industrial use was developed. It is extremely robust and can be used in the form of a hand held "dip stick".
A single screaned lead connects the unit to the electronics, which is completely isolated from the liquid by the bulkhead, therefore exluding any possibility of an electrical harzard.

Measurements have been made on a wide range of liquids and the results obtained have good reproduceability. The heaviest liquid measured is glycerol at 2°C. It is visualised that users will calibrate the individual units using thick liquids of their choice, and when suitably calibrated the transducer can be used to measure the proportions of the liquid mixtures.

The measurements obtained are generally better with the low sensitivity stainless steel fork (fork #3) developed.

Lastly the measuring instrument can be improved by automating it, where the cell phone type unit can be used for data display.

DECLARATION

This thesis could not have been carried out without great help and support from my supervisor Prof Bell as mentioned in the acknowledgement. I would like to make it clear that the breakdown of work on various sections of this thesis was as follows.

Literature review and discussion of relavant theory

Everything in this chapter is due to my own research except the equivalent circuit of the transducer which was the help of Prof Bell.

Development of transducers

I initially used some of Prof Bell's transducers, thereafter I developed some forks that were used for the measurements in the later stages of the project.

Electronics

The electronics circuit built is my work, but Prof Bell was always available for advice.

Results of the experiments

Prof Bell helped me with the the verification of my results, just to see that my results were correct.

Signature : .....

Date : 29 September 2000

TABLE OF CONTENTS

Acknowledgements i

Synopsis ii

Declaration iv

Table of Contents v

List of Illustrations viii

Chapter 1: Introduction 1

Chapter 2: Literature Review and Discussions of the Relevant Theory 3

2.1 Tuning fork's application as a vibrating transducer 3

2.2 Magnetostriction and its effects 4

2.3 Damping on the tuning fork 6

2.3.1 Hydrodynamic effect 6

2.3.2 Acoustic radiation 7

2.3.3 Viscous effect 7

2.4 Analysis of a linear system and the logarithmic decrement's measument 9

2.5 Q Factor measurement and fork's geometry 13

2.6 Electrical modelling of the transducer 15

2.7 Analysis of the tuning fork system 16

2.8 Behaviour of the equipment used 22

2.8.1 Electrical connections 22

2.8.2 Bonding 23

2.9 Choice of material 23

Chapter 3: Experiments carried out on the transducer 24

3.1 Procedure of the experiment 24

3.1.1 The relay function 24

3.1.2 Alternative Method to the relay function 25

3.2. Resonance setting 27

3.3 Magnetic biasing 27

3.4 Final transducer design 28
3.5 The perfomance of the fork is affected by its geometry and density 29

Chapter 4: Drive – Listen System 31
4.1 Features of the electronic circuitry used 31
4.1.1 Power Supply *31*
4.1.2 Isolation of the tuning fork *31*
4.1.3 Drive circuitry (see figure 4.1) *31*
4.1.4 Listen circuit *32*
4.1.5 Control circuit *32*
4.2 Features of the final electronic circuitry 33
4.2.1 Control and timing circuitry *33*
4.2.2 Drive circuit *33*
4.2.3 Transducer coil *34*
4.2.4 Listen circuit 36

Chapter 5: Measurements carried out in the project 38
5.1 Testing of the drive – listen sytem 39
5.2 Loading effects on a vibrating transducer 40
5.3 Mass calibration of various transducers 42
5.4 Transducers energy conversion from electrical – Mechanical 44
5.5 Evaluation of high and low sensitivity transducers in liquids 46
5.6 Damping of the forks vibrations in liquids is due to both the liquid's density and viscosity 49
5.6.1 Resonant frequency drops as the loading increases *50*
5.6.2 The loss loading is inversely proportional to temperature in thick liquids *51*
5.7 Oil measurement 52
5.8 Glycerol measurements 54
5.8.1 Transducer vibrations increase with an increase in temperature 56
5.8.2 Frequency changes due to temperature 58

Chapter 6: Conclusions 60

Chapter 7: Recommendations 62

Bibliography 63

Appendices 65

Appendix A: Data of various transducers used in different liquids

Appendix B: Solatron transducers

Appendix C: Transducers used in the thick liquid measurements

LIST OF ILLUSTRATION S

LIST OF FIGURES

Figure 1.1 The digital scope shows the drive – listen feature of the measurement, on the digital scope the large burst is the drive and the listen signal is between the bursts. 1

Figure 2.1 Photograph of some of the various designs of tuning forks used in the development stages. 3

Figure 2.2 Diagram shows the different parts of the tuning fork. The field from the coil make the strips vibrate longitudinally, flexing the tines. Amplitude is at peak at the fork's resonance. The resonance characteristics gives the analyses in terms of the liquid. 4

Figure 2.3 Diagram shows the change in length with the applied field in case of a biased excitation. The Iron-Nickel alloy gives the maximum magnetostrictive effect [9]. 5

Figure 2.4 Diagram shows the movement of fluid between the tines of a vibrating tuning fork. The pumping action is e/(dρ) hence the smaller the gap between the tines is, the greater will be the velocities and the greater the sensitivity to mass and viscous loading. 6

Figure 2.5 Output signal of a tuning fork driven in air, shows a very low energy loss (Q=1047) 8

Figure 2.6 Output signal of a tuning fork driven in oil shows a very rapid energy loss. Q can be derived directly from this waveform (Q=52) 8

Figure 2.7 Mechanical lumped circuit model of the tuning fork. The loss R, combined that of the fork and the liquid. The mass M, includes the inertial loading of the liquid. 9

Figure 2.8 This diagram shows the wavform of the typical exponential decrement to be obtained once the driving force is removed. 10

Figure 2.9 This diagram shows how a log decrement is used to find Q. 11

Figure 2.10 The principal amplitude frequency spectrum of a transducer driven by a continuous wave. The response to a burst is the decrement shown in figure (2.7). 14

Figure 2.11 Lumped electrical circuit model of a tuning fork. The inductance corresponds to inertia, capacitance to stiffness and the resistance to the energy dissipated [4]. 15

Figure 2.12 The practical circuit of the drive-listen system. The mechanical switch is synchronised to the on/off of the square wave drive. 16

Figure 2.13 The equivalent circuit. The primary is the electrical drive coil and the secondary is the electrical equivalent of the resonance of the fork. M represents the magnetostrictive coupling. 17

Figure 2.14 The coupling co-efficient "k" is found from the slope of the line drawn as shown by equation (2.16). 20

Figure 2.15 The diagram above shows the acoustic response and the voltage as a function of frequency as it is swept through resonance. 20

Figure 2.16	The amplifier circuit used to calculate the internal resistance (R_o) of the various forks.	22
Figure 3.1	Block diagram of a "Gunther" relay method.	25
Figure 3.2	Block diagram of the drive-listen signal (D and L) showing the burst signal as seen on the digital oscilloscope.	26
Figure 3.3	A section showing the fork interface to the liquid, with the m/s strips and their attachments to the tines. The laminations stop short of the root. The magnet was positioned to give maximum signal and the immersion of the tines can be seen.	28
Figure 3.4	The diagram shows the physical dimensions of a typical tuning fork used.	29
Figure 4.1	Voltage drive circuit. The low impedance load requires the low impedance drive.	35
Figure 4.2	Current drive circuit. The collector gives a push-pull current drive to the coil which flaty tuned.	36
Figure 4.3	Listen circuit. The low source impedance of the unit leads to a listen signal.	37
Figure 5.1	The diagram shows the acoustic signal and the output decrement on the listen phase. The drive signal can be up to 40V and the listen signal as low as 2mV (86 dB).	39
Figure 5.2	The decrement falls fast in a thick oil compared to when in water and air. The graph show the slope of the waveforms from which Q is calculated. N represents the numer of oscillations.	40
Figure 5.3	This diagram shows the set up used for mass calibration of various transducers. The acoustic signal was used to compare the efficiency of these transducers during the development stages.	42
Figure 5.4	The drive voltage V_{coil} is obtained from the burst signal and the amplified listen signal V_0 is the maximum signal of the decrement.	44
Figure 5.5	This graph shows V_{coil}/V_0 plotted against the loss (1/Q). The best transducer from these results is S.Steel A with the lowest loss angle and the lowest V_{coil}/V_0.	45
Figure 5.6	An overview of the transducer performances.	49
Figure 5.7	The frequency decrease is high when measuring high density liquids.	51
Figure 5.8	Decrements obtained for oil heated from room temperature to 54 °C. At higher temperatures the decay is lower than at lower temperatures.	52
Figure 5.9	The logarithmic plots drawn show the decrease in slope as the temperature increases. The Q factor obtained is equal to π/slope.	53
Figure 5.10	The output voltage increases as the temperature of glycerol rises.	56
Figure 5.11:	The loss angle decreases by about 0.0008 per °C increase in temperature. As the liquid becomes thinner the vibrations become larger and last longer.	56
Figure 5.12	The loss in glycerol with a light sensitive aluminium fork decreases by about 0.0009 per ^{0}C increase in temperature.	57

Figure 5.13 The loss angle decreases as the temperature increases. The loss per °C is more in a light fork (fork #6) than in a heavy fork (fork #7). 57

Figure 5.14 The resonant frequency of a heavy fork (fork#1) stabilises faster than that of a light fork (fork#3) when driven in glycerol at low temperatures. 58

Figure 5.15 The resonant frequency stabilises faster with a heavier fork (fork #7) than with a light quartz fork (fork #6) 59

LIST OF TABLES

Table 2.1 The coupling co-efficient "k" for fork #1 is obtained using the information given below. 19

Table 2.2 The coupling co-efficient "k" for AL 2 is obtained using th einformation given below. 19

Table 3.1 This table shows the physical dimensions and the various mateirals of the forks used. 29

Table 4.1 This table shows that various forks have different gain due to their R_0 values obtained using equation (2.18) 37

Table 5.1 The fall in frequency for water is greater than the fall for oil since water has a greater density. The loss however is greater for the thick oil. 41

Table 5.2 The sensitivity of the various forks used was obtained by mass calibration. F_i is the frequency measured without the added mass, whereas F_m is that with the added mass. 43

Table 5.3 This table shows the relationship of V_{coil}/V_0 as plotted against the loss angle (1/Q) for various forks operating freely in air. The losses in air are due to the internal losses of the forks. 45

Table 5.4 A low sensitive fork (fork # 1) was driven in various liquids (water, paraffin, engine oil and glycerol) and due to its good coupling good measurements were obtained in very thick liquids. 46

Table 5.5 A high sensitive fork (fork # 6) was driven in various liquids (water, paraffin, engine oil and glycerol) and it also has a good coupling enabling the transducer to be used for measurements in thick liquids. 47

Table 5.6 A low sensitive fork (fork # 3) was driven in various liquids (water, paraffin, engine oil and glycerol) and it also has a good coupling enabling the transducer to be used for measurements in thick liquids. 47

Table 5.7 A high sensitive quartz fork (fork #6) driven in hot oil. 54

Table 5.8 A low sensitive brass fork (fork #7) in hot oil. 54

Table 5.9 The data for fork#3 driven in cold glycerol is displayed below. 54

Table 5.10 The data for fork #1 driven in glycerol is displayed below 55

CHAPTER 1

INTRODUCTION

This report discusses in detail all the work carried out to reach the main objective of this project, which was to classify heavy fluids using a vibrating transducer, namely a tuning fork. The main properties looked at in these fluids are viscosity and density, and they are measured using the instruments shown in figure (1.1). These properties are related by the loss angle and the frequency decrease measured.

It was thus realised that with the technology now available, these prperties can be simply and reliably measured. So the production of a portable instrument in a form of a "dip stick" was explored for general classification of liquids.

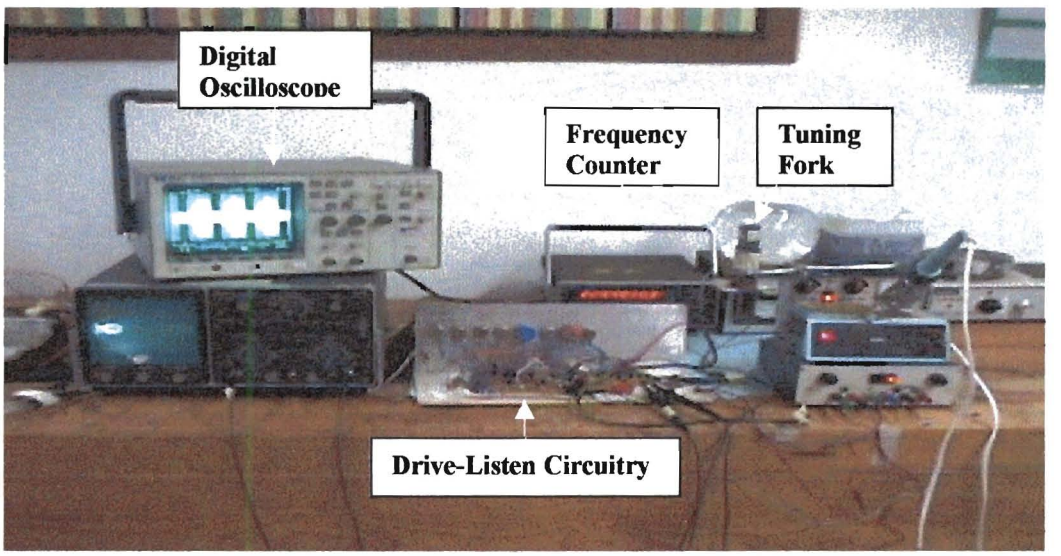

Figure 1.1: The digital scope shows the drive-listen feature of the measurement. On the digital scope, the large burst is the drive and the listen signal is between the bursts.

When driven in a fluid the transducer drives the liquid and the added mass of the system reduces the frequency [8].

This occurs irresepective of the viscosity and at high viscosities, there will be a further added mass due to the viscous drag of the liquid [16].

The tuning fork designed was driven magnetostrictively as described in section (2.2) and was set to vibrate at its resonant frequency. The natural resonant frequency of the transducer depends on the mass loading of the liquid surrounding the element while the decrement of the vibrations depends on the energy loss.

By observing the decay in the vibrations when the drive is switched off, the energy losses can be measured. The Q factor, a measurement widely used in electronics can be obtained from the decrement. The inverse of Q is the energy loss angle, and in the low to medium viscous liquids it has a first order relationship to viscosity. With very thick liquids this instrument is designed to measure, the parameter change in ferquency and loass angle can be considered as characterising the liquids.

The phenomena of thixotropy became evident for these heavy liquids. As developed here, the instrument is intended for general manual use where the fork is part of a "dip stick" giving mass loading and the loss angle of the liquid sampled.

The resonant frequency is maintained and any change is detected and used to derive the change in density of the liquid. Density and viscosity are proportional to the product of the fluid velocity and the geometry of the lamina of the fluid trapped between the tines [9]. The electronic circuitry built helps maintain a high Q, hence a good perfomance by the transducer.

CHAPTER 2

LITERATURE REVIEW AND DISCUSSION OF RELEVANT THEORY

This chapter focuses on the relevant theory that relates to this thesis project. The theory is a summary of information taken from journals, some practical experience, the internet and texts listed in the bibliography.

2.1 TUNING FORK'S APPLICATION AS A VIBRATING TRANSDUCER

Tuning fork is a vibrating body and was used as a transducer in this project. A wide range of tuning forks (shown by figure 2.1) of different materials (i.e. aluminium, glass, stainless steel and fused quarts) and different mechanical designs were used, and they each resembled the diagram on figure (2.2). They all had biasing magnets attached. Some had their tines nickel-plated or had nickel strips glued to their sides and had coils of copper wire wound around them.

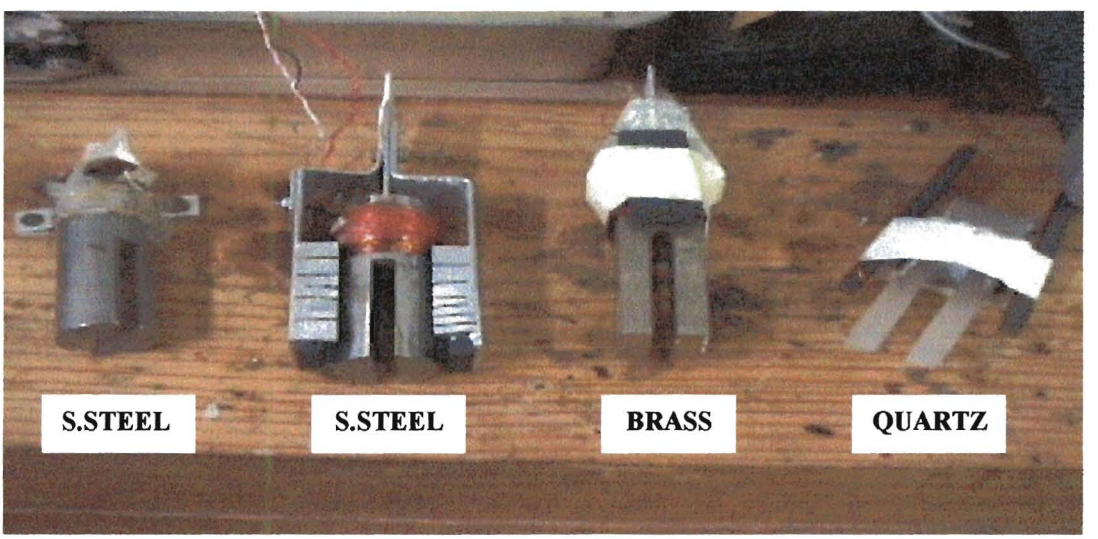

Figure 2.1: Photograph of some of the various designs of tuning forks used in the development stages (see appendix C for the improved transducers).

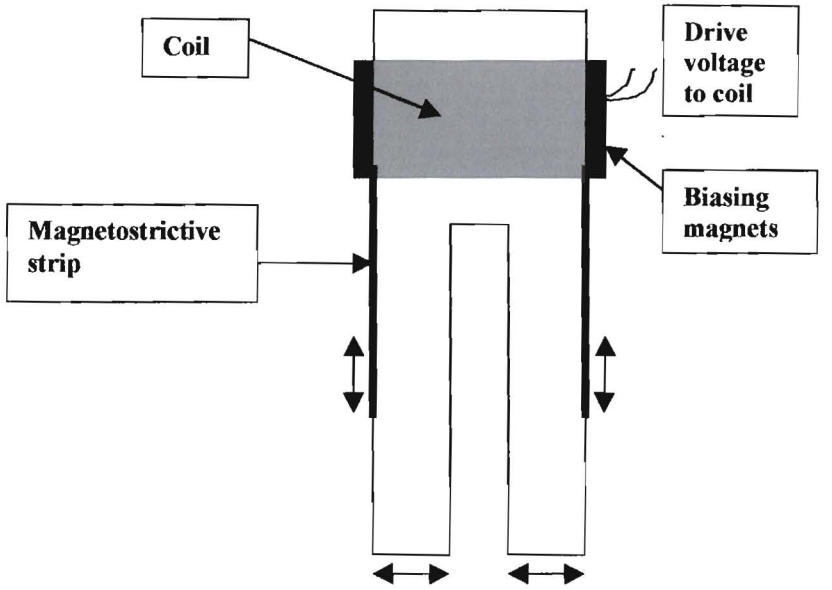

Figure 2.2 Diagram shows the different parts of the tuning fork. The field from the coil makes the strips vibrate longitudinally, flexing the tines. Amplitude is at peak at the fork's resonance. The resonance characteristic gives the analyses in terms of the liquid.

The "burst" drive signal is connected to the coil, and the tuning fork is set into resonance. In the listen mode the vibrations of the tuning fork are translated to an equivalent electrical signal, shown as a decrement from which Q was obtained. The technique that links the mechanical and the electrical characteristic of the tuning fork is called magnetostriction.

2.2 MAGNETOSTRICTION AND ITS EFFECTS

If a magnetic field is applied to a magnetostrictive material, that material will experience a small change in dimensions and this change will be in parallel to the magnetic field as shown in figure (2.2) [4]. Similarly a change in the dimensions of the material caused by some mechanical stress, will result in the generation of a magnetic field (shown in figure 2.3).

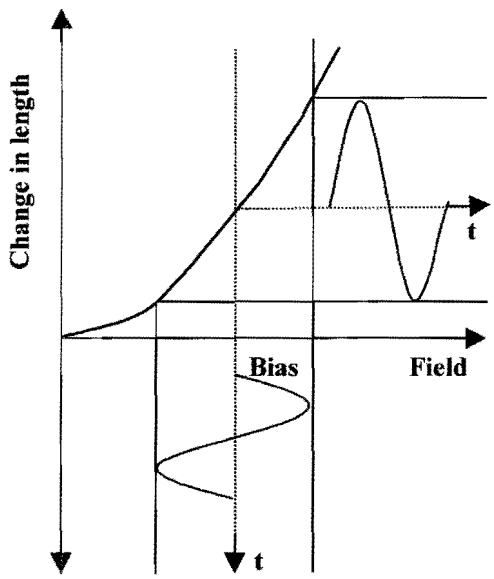

Figure 2.3: Diagram shows the change in length with the applied field in case of a biased excitation. The Iron-Nickel alloy used gives the maximum magnetostrictive effect [9]

Different materials respond differently to the magnetic field applied. So when magnetostriction occurs, the magnetostrictive strips change more than the remaining structure of the tuning fork material. As a result the bimetallic effect takes place and the tines start bending.

As soon as the electrical signal is removed, the tines revert to their natural free frequency [3]. It can thus be seen that if the electrical signal is applied to the coil, the tines will follow the oscillating magnetic field. Consequently due to the reverse effect, a physical movement in the tines will in general be reproduced in the form of a voltage across the coil.

During magnetostriction, eddy currents and hysteresis losses occur and may lead to the increase of temperature of the fork. As a result a temperature sensor (LM35) was attached to the transducer to monitor its temeprature changes.

2.3 DAMPING ON A TUNING FORK

When a vibrating tuning fork is immersed in a fluid, there will be some energy dissipation in a form of viscous losses, hydrodynamic and acoustic radiation as discussed below. When these losses are high, they can reduce the sharpness of the resonance and consequently the frequency stability, which ultimately affects the resolution of the instrument. These losses were however useful in the classification of the transducers in the development stages.

2.3.1 HYDRODYNAMIC EFFECT

When a tuning fork vibrates in a liquid as shown by figure (2.4) below, it imparts kinetic energy into that liquid and sets it in motion [17]. In turn, an inertial mass loading is experienced by the tuning fork, thus increasing its static lumped mass parameter. As a result the resonant frequency of the tuning fork in that medium is lowered.

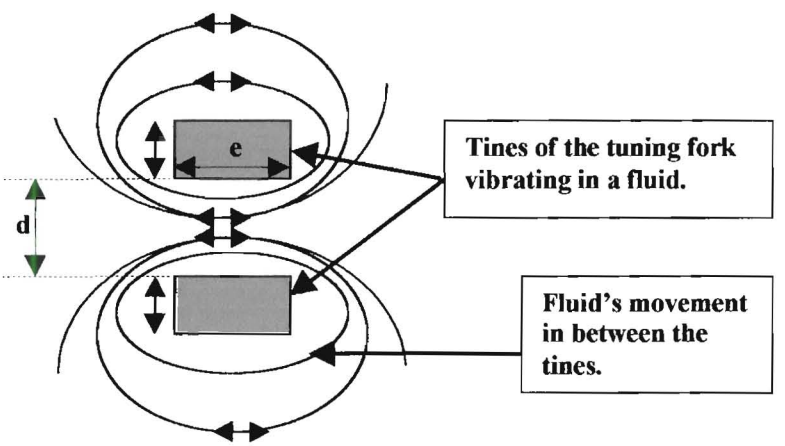

Figure 2.4: Diagram shows the movement of fluid between the tines of a vibrating tuning fork. The pumping action is e/(dρ) hence smaller the gap between the tines is, the greater will be the velocities and the greater the sensitivity to mass and viscous loading.

The movement of the fluid between the tines imposes an extra loading on the tuning fork due to the viscous nature of the fluid concerned. This damping effect is, small in lighter fluids (e.g. Water) than in heavier fluids (e.g. Oil). Because the laminar of the fluid trapped between the tines cannot escape immediately, there is an increase of pressure in the film, which imposes an elastic force on the system. This behaves as a stiffness phenomenon and serves to raise the resonant frequency. The total effect of this reactive loading depends on their magnitudes.

2.3.2 ACOUSTIC RADIATION

When a tuning fork vibrates in a fluid, some energy is radiated in the form of sound. These acoustic energy losses are negligible compared to the losses in the liquid. In the development stages the efficiency of the various forks was obtained by comparing the sound signals picked by a microphone, and these signals were found to be a measure of i_2 as shown in figure (2.13).

2.3.3 VISCOUS EFFECT

Vibration of the transducer in a liquid (as seen in figure 2.4) induces viscous drag forces, which present a damping effect. This phenomenon can be reduced or enhanced by choosing the geometrical design that will either maximise or minimise the shearing forces [17]. By observing the output signals shown in figure (2.5 and 2.6) obtained when driving the tuning fork in Air and Oil, the Q factor dropped as a result of the viscous loading. Therefore liquids with higher viscosities present a higher loss loading to the transducer, as shown by the drop in the Q factors in figures (2.5 and 2.6).

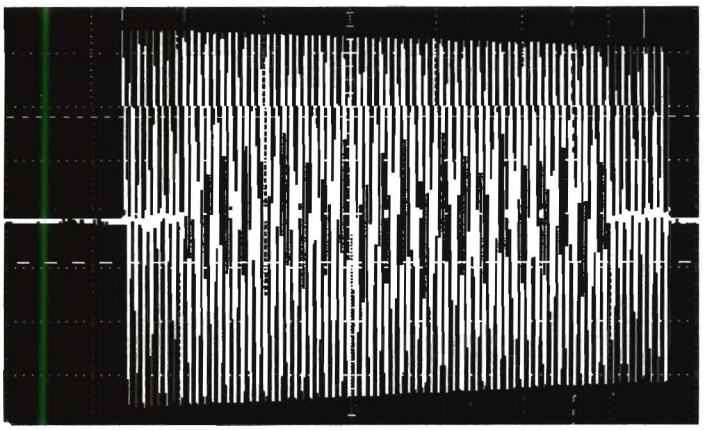

Figure 2.5: Output signal of a tuning fork driven in Air, shows a very low energy loss (Q=1047).

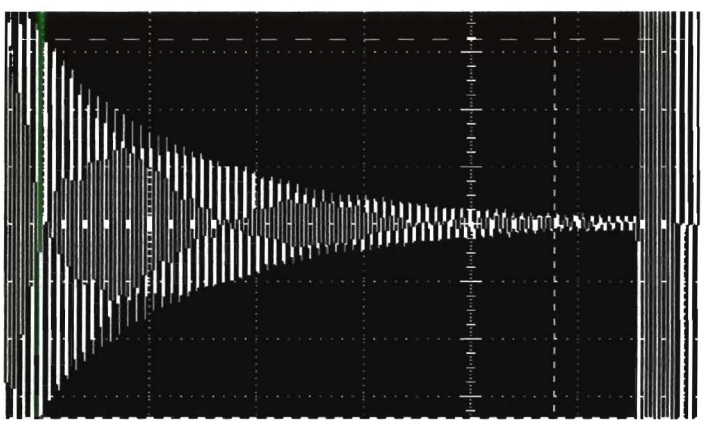

Figure 2.6: Output signal of a tuning fork driven in Oil, shows a very rapid energy loss. Q can be derived directly from this waveform (Q=52).

Figure (2.5) shows a high Q signal obtained when the fork is driven in a low loss medium (i.e. Air) while figure (2.6) shows a low Q signal obtained in a heavily damped medium (i.e. Oil). The damping experienced by the transducer is due to both the loss and the mass loading of the fluids under examination.

2.4 ANALYSIS OF A LINEAR SYSTEM AND THE LOGARITHMIC DECREMENT'S MEASUREMENT.

It is useful to model the structure as a 1st order linear system and to derive the differential equation of motion by applying Newton's second law if an analytical approach is to be adopted [17].

Take an ideal system made of lumped parameters and exhibiting a single degree of freedom figure (2.7).

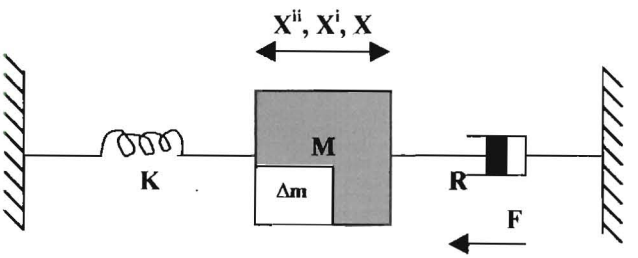

Figure 2.7: Mechanical lumped circuit model of the tuning fork. The loss R combines that of the fork and the liquid. The mass M includes the inertial loading of the liquid.

Where such a system has:

In general the stiffness of the spring is a constant (k), but in thixotropic liquids it changes, mass (M) and viscous damping (R). Applied force (F), displacement (x), velocity ($x^{!}$), acceleration ($x^{!!}$). Δm is the small additional mass attached to the tuning fork's tines.

In reality these parameters are distributed and not purely lumped. However, valuable insight can be obtained from this simplified model.

When there is damping, the generalized equation of motion is given by:

$$Mx^{!!} + Rx^{!} + kx = F\sin\omega_o t \qquad (2.1)$$

$$\omega^2 Mk = 1 \qquad (2.2)$$

From equation (2.2) above, the relationship between mass and frequency is given by the equation:

The fractional change in mass = 2 (fractional change in frequency) (2.3)

In the tuning forks used in this project, the mechanical resistance R is kept very small, hence $\omega^2_o > \alpha^2$ making s complex and β imaginary as given below.

$$\beta = j\sqrt{[\alpha^2 - \omega^2_o]} = j\omega_d \quad (2.4)$$

Where: $w_d = w_o\sqrt{[1- \xi^2]}$, and is the angular frequency of the damped free oscillations. Therefore for slight damping or low values of internal friction, the damped frequency is nearly equal to, although slightly less than the undamped natural frequency. $\xi = R/(2M\omega_o)$ is the viscous damping factor, $\alpha = (R/2M)$ is the loss and $\omega_o = \sqrt{(K/m)}$ is the natural free resonant frequency. Quality factor ($Q = 1/2\xi$). Note that M is proportional to $\mathbf{1/f^2}$.

Another form of analysing the system is by a decaying sinusoid shown by (fig 2.8).

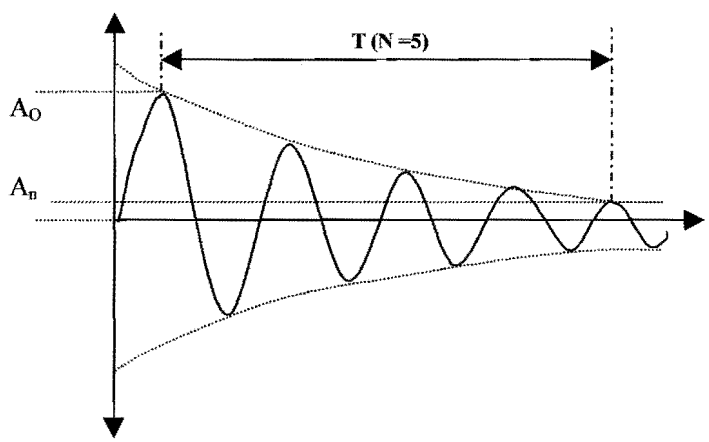

Figure 2.8: This diagram shows the waveform of the typical exponential decrement to be obtained once the driving force is removed.

The sinusoid above is represented by equation (2.5) where $\mathbf{A_o}$ is the amplitude of the signal at the start of the decrement and $\mathbf{A_n}$ is the signal at the $\mathbf{n^{th}}$ cycle taken.

$$x(t) = A_o \, Sin\omega t \qquad (2.5)$$

The frequency of the decrement is very close to the natural frequency of the system [3], and from the decrement the loss term can be obtained. The method described by figure (2.8) where the amplitude against frequency characteristics of the system are shown, is one form by which the Q (quality factor) is obtained when using equation (2.6) below.

$$Q = \pi n / \ln (A_o/A_n) \qquad (2.6)$$

Q values were also accurately obtainable by plotting the log of the amplitude against the number of oscillations. The result is a straight line where the slope is proportional to the loss angle (loss = slope/π) and the Q is given by π/slope (see figure 2.9).

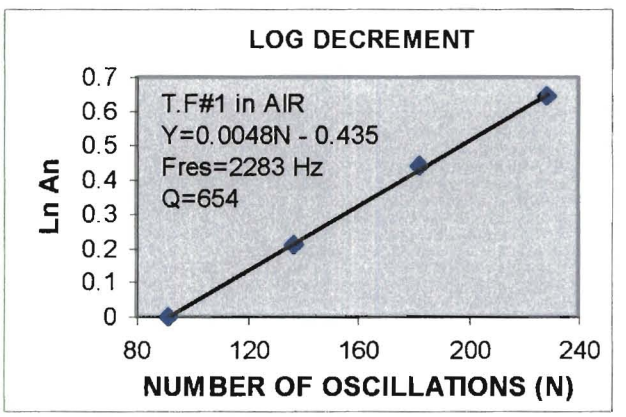

Figure 2.9: This diagram shows how a log decrement is used to find Q.

Figure (2.9) shows the logarithmic plot of a tuning fork driven in air. The slope is given as 0.0048 (shown by equation 2.7) while the corresponding Q=654 (shown by equation 2.8).

$$\text{Ln } A_n = \text{Ln } A_o - \pi n/Q \tag{2.7}$$

The Q factor of a transducer in any liquid can also be obtained from figure (2.9) above by using equation (2.8).

$$Q = \pi / \text{slope} \tag{2.8}$$

From figures (2.5 and 2.6) and equation (2.8), it is seen that the faster the decrement falls, the steeper will be the slope hence the lower the Q factor measured.

The inverse of Q, gives the *loss angle* which is a good measure of viscosity [6].

$$\text{Loss Angle} = 1/Q \tag{2.9}$$

A measure of the rapidity with which the transducer vibrations are damped by the surrounding medium, is the time taken for the amplitude to decay to **1/e** of its initial value $\mathbf{A_o}$ [17], this being the mechanical time constant of the system given by:

$$\tau = 1/\alpha = 2M/R \tag{2.10}$$

So the longer it takes the oscillations to decay the smaller mechanical resistance as shown in figure (2.5 and 2.6).

The amplitude of the tine's vibrations is proportional to the energy due to one vibration.

$$E \propto A^2 \tag{2.11}$$

The loss angle is directly proportional to the energy dissipated, therefore the viscosity is directly related to the energy dissipated.

Viscosity = f (energy dissipated) **where**: f is some function

$$\text{or Viscosity} = f_2 \text{ (loss angle)}$$

$$\text{or Viscosity} = f_3 [\ln(A_o/A_n) / \pi n] \quad (2.12)$$

The energy stored in the fork is proportional to its density, and the loss is purely a function of the fork's geometry[9]. As a result stainless steel is used for measurements in very heavy liquids and aluminium for simple liquids.

$$E_{stored} = \tfrac{1}{2} Mv^2 = \tfrac{1}{2} k\rho v^2 \quad (2.13)$$

2.5 Q FACTOR MEASUREMENT AND THE FORK'S GEOMETRY

Q factor can easily be defined as the total energy stored in the structure divided by the sum of the energy losses from the tuning fork per cycle [6].

$$Q = 2\pi(\text{Energy stored}) / (\text{Energy lost per cycle}) \quad (2.13)$$

A high Q factor is desirable because it simplifies the feedback control electronics since a high degree of phase shift stability is not imperative, and it also minimises the perturbing effect of the drive electronics and gives a high resolution. It also implies a very low unwanted coupling to the external world, which gives high accuracy and long term stability. As a result, a tuning fork of good design is necessary for a high Q to be maintained.

A high Q factor of the resonator means that the sensor performance is almost entirely dependent on the mechanical properties of the tuning fork.

When the forks are designed to couple strongly with the liquid by making the gap between the tines small, the sensitivity becomes high but the measurements are restricted to thinner liquids (see table 4.2). Therefore a fork designed to have a very low coupling to the liquid would work well in thick liquids.

The bandwidth method described below is one form of measuring Q, suitable for heavily damped systems with a low quality factor. With the the broad bandwidth technique the frequency can be accurately measured, however the decrement method also gave good reproduceable results.

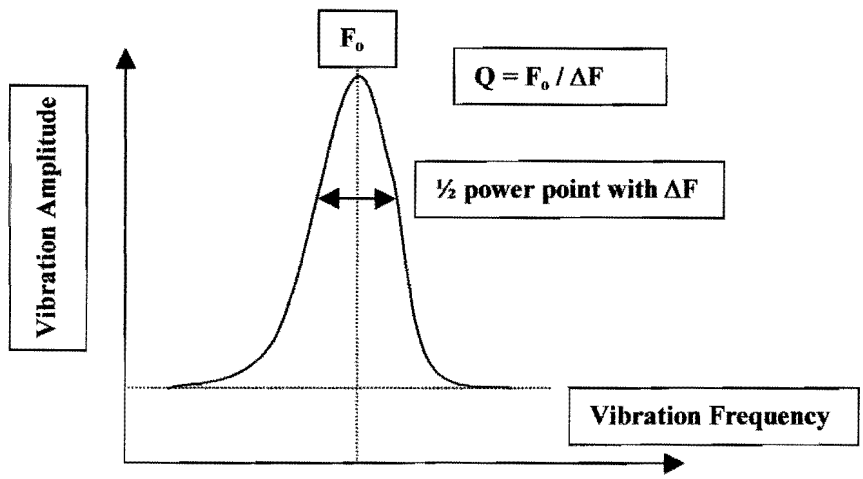

Figure2.10: The principal amplitude frequency spectrum of a transducer driven by a continuous wave. The response to a burst is the decrement shown in figure (2.7).

$$Q = F_o / \Delta f \qquad (2.14)$$

$$F_o = k\, t\, \sqrt{(E / \rho)} / l^2 \qquad (2.15)$$

Where: t and l are the thickness and the length of the tines respectively. F_o is the fork's natural frequency, E the elasticity modulus of the material, ρ the density of the fork's material used. Lastly k is a constant depending on the geometrical shape of the fork. $\Delta f = F_2 - F_1$ where F_2 and F_1 are the half power frequencies.

In this project however, the method described by figure (2.9) was used for the Q measurements. With this method the Q factor is determined by electronically shutting off the driving force within a number of decay transients, so as to leave the system in free vibrations. The decrement is then analysed as shown by figures (2.8 and 2.9) and then Q is obtained.

From equation (2.15) it is seen that when the frequency of a certain type transducer is measured, the factor k in the equation can be calculated and combined with $\sqrt{(E / \rho)}$ and written as a dimensionless constant K as shown in figure (2.14).

Equation (2.15) also shows that the frequency of the forks with the same shape and material vary as their linear dimensions. The frequency is seen to be inversely proportional to the tine's length and directly proportional to the tine's thickness and is independent of the width [9].

2.6 ELECTRICAL MODELLING OF THE TRANSDUCER

Tuning forks used in this project can be modeled electrically.

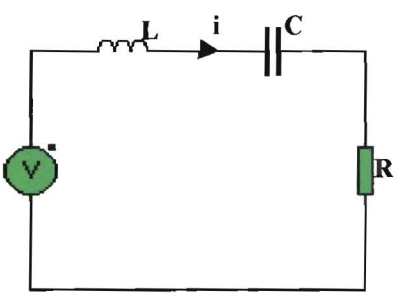

Figure 2.11: Lumped electrical circuit model of a tuning fork. The inductance corresponds to inertia, capacitance to stiffness and the resistance to the energy dissipated [4].

Where: The inductance L represents the mass "M", capacitance C represents coil

stiffness "K". The resistance R viscous damping "R".
The physical properties of the tuning fork and surrounding fluid in which it is immersed are transformed into equivalent impedances, which will affect the input voltage. The loading due to the liquid examined is a source of resistance.

The coil wound round the fork, couples magnetostrictively to the fork and this is represented in the equivalent circuit as a mutual coupling between the two inductors.

2.7 ANALYSES OF THE TUNING FORK SYSTEM

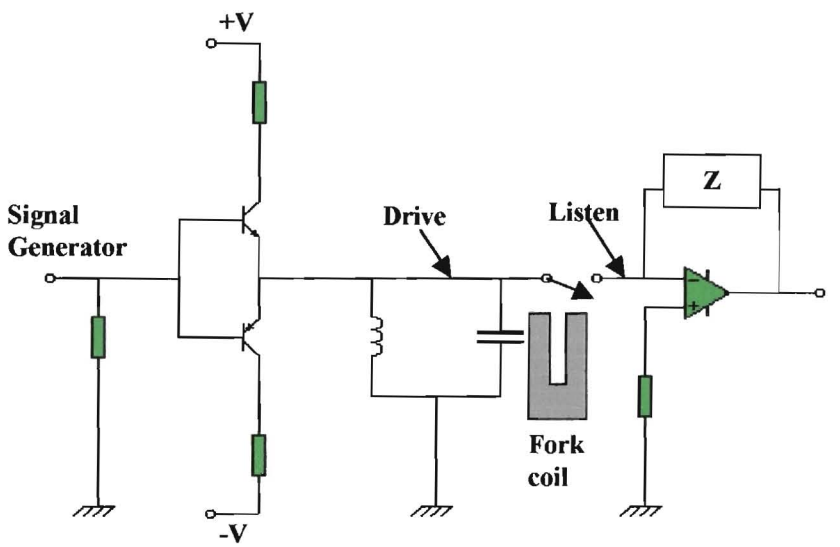

Figure 2.12: The practical circuit of the drive-listen system. The mechanical switch is synchronised to the on off of the square wave drive.

The coil of the fork is permanently connected to the drive collectors. On the listen mode, the square wave signal is off and the coil is switched to the listen position. The heavy drive current does not go through the switch and the transistors do not load the input to the listen amplifiers.

A simple transformer is used as an equivalent circuit shown by (Figure 2.13).

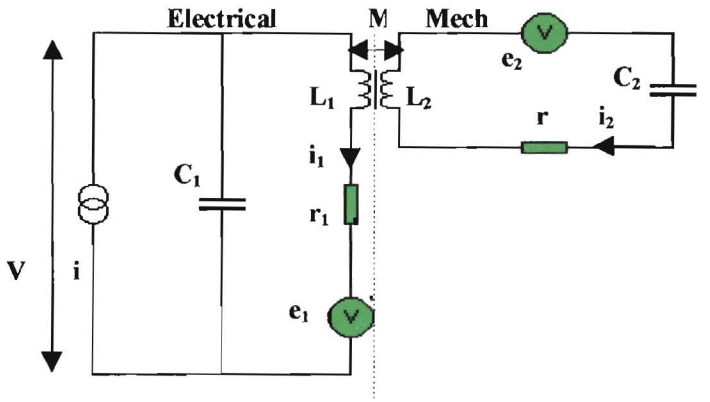

Figure 2.13: The equivalent circuit. The primary is the electrical drive coil and the secondary the electrical equivalent of the resonance of the fork. M represents the magnetostrictive coupling.

The circuit above shows the primary as being electrical and being mutually coupled to the secondary, which is the vibrating tines. The series L_2C_2r are the equivalent of the lumped mass, stiffness and loss of the actual fork.

The vibration at the end of the tines is a maximum and this was selected to compare to i_2. The ratio of current i_1 to the tine velocity gives the electrical to mechanical coupling and it can be observed by measuring the tine amplitude and the current i_1. The signal on a microphone placed just below the tines picks up the vibration i_2 very strongly and was extremely used in optimising such parameters as the DC bias and the primary circuit design.

The circuit is current driven and thus when off, it conveniently represents an open circuit for the listen phase. The current drive i_1 is fixed, and the voltage V changes. The capacitive tuning of the low impedance coil increases it to 10 or 20 ohms, allowing a higher drive current. By limiting the bandwidth also improved the quality of the waveforms.

In the absence of a liquid the secondary is sharply tuned and r is small. Most of r originates in the magnetostrictive drive strips and a larger r was acceptable to obtain a strong drive for the thick liquids.

e_1 is reflected from the secondary and is small compared to the drive voltage. e_1 is the " back emf " so called as it is negative $e_1 = -(\omega M i_1)/Z$. Analysis shows that $e_1 = (\omega^2 M^2 i_1)/r$ at resonance. Substitution of $k^2 L_1 L_2$ for M^2 and Q for $\omega L_2/r$ gives $e_1 = (k^2 Q \omega L_1) i_1$.

When driven by a continuous wave, e_1 is not observable, but by square wave modulating the drive (the drive-listen cycle) only e_1 is present on listen, and it has the characteristic decrement of the resonance and thus can be amplified and measured using a digital storage scope. In the listen mode, e_1 starts at the value given in this equation and decays exponentially and can be measured reasonably well.

There is however a switching transient as seen in figure (4.4), which intrudes on the first cycles of the decrement. The drive voltage across the coil is taken as $\omega L_1 i_1$ although it is somewhat less because of r_1. Equation (2.16) is then obtained and a precise value for Q is obtained from the decrement [4].

$$V/ e_1 = 1/(k^2 Q) \qquad (2.16)$$

In this form the terms are large for the high loss liquids of interest. This equation was used as an overall test of the validity of the equivalent circuit by measuring a range of liquids, going from low loss water and paraffin to high loss car oil and glycerol. Two forks were used stainless steel designed for heavy liquids and aluminium, which gives a higher sensitivity but not the full loss range.

Comprehensive measurements are given in the accompanying tables. They are followed by two graphs using equation (2.16) from which the magnetostrictive coupling co-efficient (k) was obtained.

Table 2.1: The coupling coefficient "k" for fork#1 is obtained using the information given below.

STAIN LESS STEEL FORK#1					
	AIR	WATER	PARAFFIN	ENGINE OIL	GLYCEROL
Vcoil	0.281	0.47	0.613	0.65	0.7
Vo	12.59	8.75	9.375	2.422	1.238
e1	0.067	0.046	0.050	0.013	0.007
Vcoil/e1	4.218	10.152	12.358	50.723	106.866
Frequency	2284	1870	1935	1889	1777
Q	1054	303	244	54	28
1/Q	0.0009	0.0033	0.0041	0.0185	0.0357

Table 2.2: The coupling coefficient "k" for AL2 is obtained using the information given below.

ALUMINIUM FORK (AL2)					
	AIR	WATER	PARAFFIN	ENGINE OIL	GLYCEROL
Vcoil	6.375	7.44	7.81	7.44	7.06
Vo	8.625	13.9	12.2	5.5	4.719
e1	0.025	0.040	0.035	0.016	0.013
Vcoil/e1	259.435	187.873	224.698	474.807	525.124
Frequency	2885	2241	2344	2283	2119
Q	142	122	117	31	21
1/Q	0.007	0.0082	0.0085	0.0323	0.0476

The drive voltage (V_{coil}) and the output signal (V_o) shown in the two tables above were measured at the fork's coil and at the output of the listen amplifier respectively. e_1 the back emf shown in the tables, was found by dividing V_o with the gain of the listen amplifier. The gain of the amplifiers depends on the inductance of the fork's coil, so the less the inductance the higher the gain.

By taking the slope of the plot of the ratio of V_{coil}/e_1 against 1/Q as shown in the graphs below, the coupling coefficient "k" of the forks described above was obtained. The k for the stainless steel fork is higher at 0.018 than the aluminium fork at 0.011, which means that the conversion of electrical ↔ mechanical energy is higher in a stainless steel fork than it is for the aluminium fork.

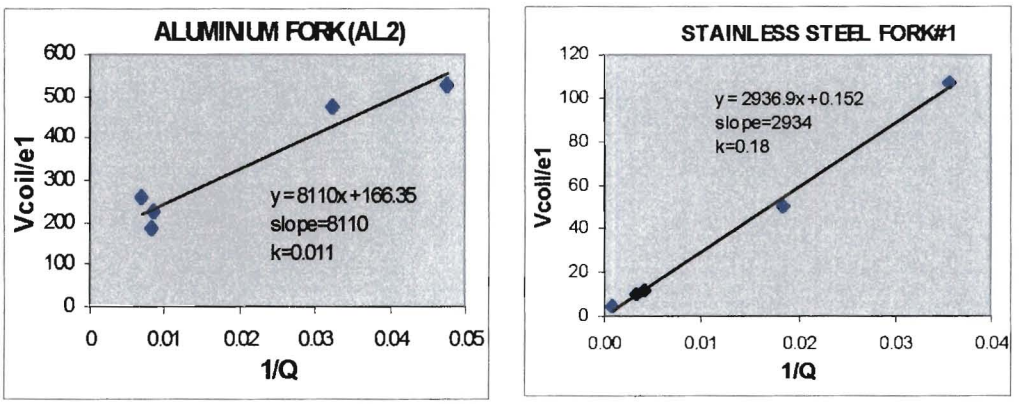

Figure 2.14: The coupling coefficient "k" is found from the slope of the line drawn, as shown by equation (2.16).

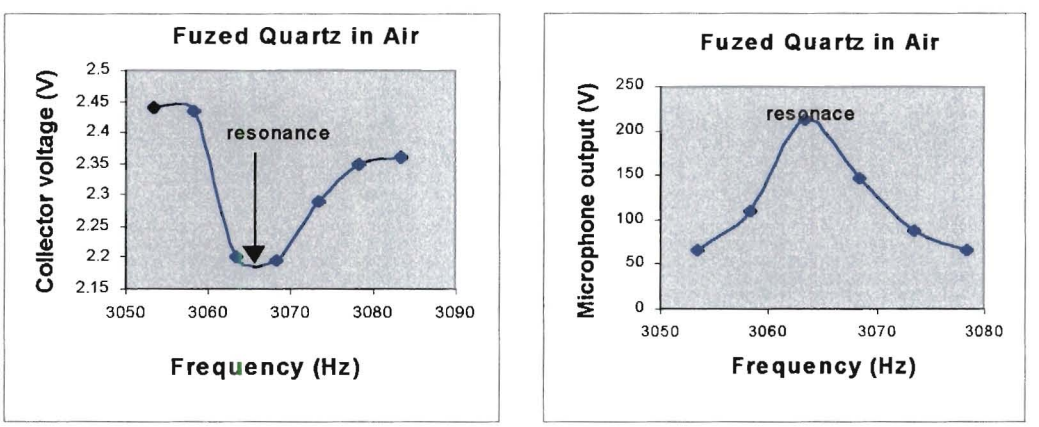

Figure 2.15: The diagrams above show the acoustic response and the voltage as a function of frequency as it is swept through resonance.

The graphs shown by figure (2.14) above show that when using a continuous wave signal, the voltage required at the collector is a minimum when the fork is at resonance and higher when on either side of resonance.

The performance of the fork is also at its best when at resonance as confirmed by the maximum sound signal picked at resonance. These graphs show that it is easier to drive the fork at resonance than when it is on either side of resonance. The back emf (e_1) from the resonance is only a small percentage of the drive voltage and this falls to a very low fraction for the low Q factors in oil and glycerol.

This was avoided by using an on/off drive having a drive listen cycle. The cycle is sufficiently long for the signals to reach a maximum. When the drive goes off only e_1 is left and it decays exponentially to zero with the current i_2.

The output signal was obtained by using an inverting amplifier shown below, since the full power of the listen signal is used. The current flows directly from the fork's coil to the opamp's feedback impedance. By connecting a 10 Ω resistor in series with the fork during the listen cycle, the fork's current and resistance can be found by using equation (2.18). Knowing R_o helps in the calculation of the gain of the listen circuit (see table 3.1).

$$\text{(Current across the fork's coil) } I_{coil} = e_1(R_o+10) \qquad (2.17)$$

$$\text{(Resistance of the fork) } R_0 = 10/(V_o/V_{10} - 1) \qquad (2.18)$$

Where: V_o is obtained without a 10Ω resistor and V_{10} is with a 10Ω resistor.

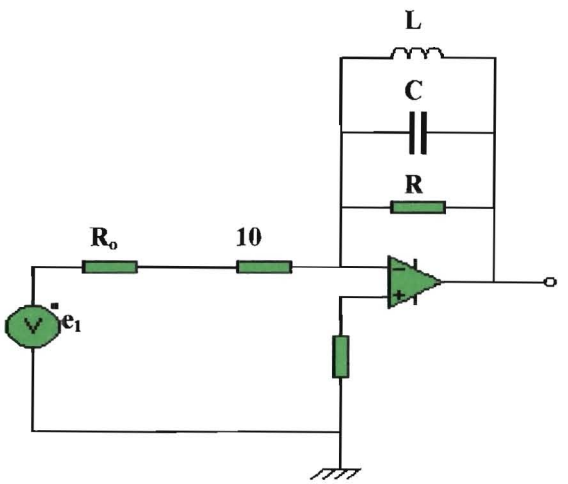

Figure 2.16: The amplifier circuit used to calculate the internal resistance (R_o) of the various forks.

2.8 BEHAVIOR OF THE EQUIPMENT USED

Besides the material and the mechanical properties of the transducers used, their performance also depends on the following physical characteristics: electrical connections, backing and bonding etc.

2.8.1 ELECTRICAL CONNECTIONS

These include the coil wound around the transducers, connections between components and any other external connections. The coil forms part of the intermediate layers placed on the transducers, so their thickness and impedance influences the sensitivity of the transducer.

The electrical tuning network together with the contact resistance and inductance of the electrical connections affect the electrical impedance of the transducer and can affect their overall sensitivity.

2.8.2 BONDING

The transducer's performance also depends on the state of the bond at the interface between the magnetostrictive strip and the tines. The magnetic field causes the strips to vibrate longitudinally in phase, making the tines vibrate in antiphase as shown by figure (2.2). Since the magnetostrictive effect is reversible, the voltage will be produced in the coil by the transfer of energy from the vibrations.

Electrical energy ↔ Mechanical energy

The coil must also be as close to the root of the fork and to the magnetostrictive strips as possible, because any improper winding of the coil will cause loss of the drive signal. This also applies to the state of the interaction between the transducer and the liquid used.

2.9 CHOICE OF MATERIAL

The material chosen is important if good temperature characteristics, low temperature coefficient [1/f (df/dθ)] and sensitivity are to be realised. In general low density materials are preferred as they allow the mass loading of the surrounding fluid to be proportionately higher.

Also a good material chosen would have a low internal friction and low temperature coefficients. Where the temperature coefficients of both the linear expansion and elasticity of the material used is small. A material with a high thermal conductivity is also important in that it ensures that thermal equilibrium is rapidly achieved. So the commercial availability of aluminium and stainless steel made them the natural choice of materials eventhough some other transducers were also explored.

CHAPTER 3

EXPERIMENTS CARRIED OUT ON THE TRANSDUCER

The main focus of this thesis was to develop a technique and an instrument to classify heavy fluids (i.e. Oils) using a tuning fork.

At the beginning of the project, a particular tuning fork referred to as fork #1 and the drive listen circuitry I previously used were still available. It is from this basis that a technique to extract the necessary information to evaluate Q was developed. As a result a great effort was put into the design of the tuning forks. The electronics was redesigned and a new drive-listen circuit was built.

3.1 PROCEDURE OF THE EXPERIMENT

Before performing the experiments, it was made sure that all the electrical interconnections were good, and that all the other equipment used functioned satisfactorily. Two methods were used, and in both cases the aim was to drive the fork with a burst signal and to obtain the decrement on the listen mode. The unit's stability was important and required clamping throughout the experiments, so it was secured well above the actual tines.

3.1.1 THE RELAY FUNCTION

In this method the circuit was connected as shown in figure (3.1) below. The burst signal was obtained by combining a clock signal and any desired square wave output from the counter through a NAND gate [22]. That burst signal would then be fed through the drive circuit. The amplitude of the burst could be adjusted to accommodate the various liquids.

For the fork to be switched from drive or listen mode, a square wave synchronous signal was used to control the "Gunther" relay thus isolating the drive from the listen cycle. The duration of the drive/listen cycle could also be controlled allowing the transducer to perform at its best. On the listen mode, the relay switches and connects the fork to the listen circuit where the output signal is amplified. As a result the decrement could be measured very precisely on the digital oscilloscope.

From there onwards the procedure was similar to the alternative method described below, and thus was finally used.

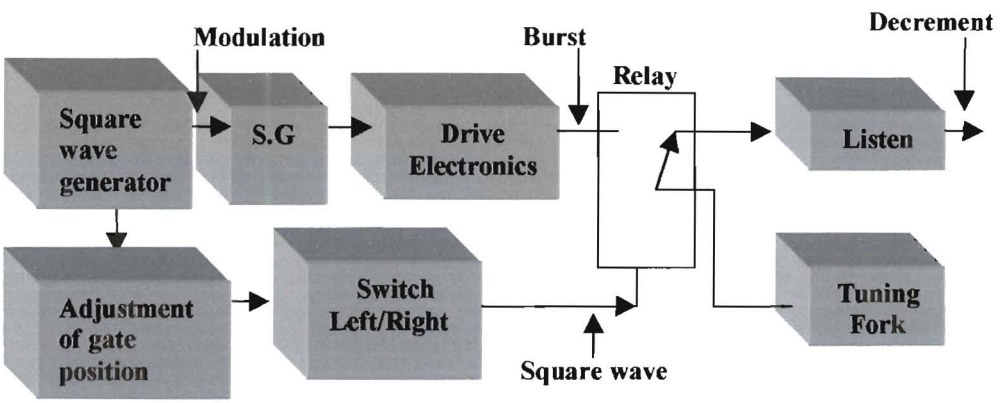

Figure 3.1: Block diagram of a gunther relay method.

3.1.2 ALTERNATIVE METHOD TO THE RELAY FUNCTION

The final circuit used was connected as shown in figure (3.2). The burst of drive oscillations was obtained by square wave modulating the signal generator. To vary the duration of the drive and burst cycles, the PRF on the square wave generator was adjusted. At low signal strength the digital oscilloscope was subject to saturation but this was avoided by using the switch at the input of the listen circuit.

The pulse generator modulates the signal generator with a square wave, giving the operator control of the drive-listen. For high Q air measurements, the PRF required could be more than a second but for high loss oil it could be as low as 20msec.

The tuning fork was driven by an amplified burst signal from the drive circuit through its coil. The amplitude of the burst could also be adjusted on the signal generator as shown in figure (3.2) below. The coil of the fork was also connected to the listen circuit through a relay switch during the listen phase. So, when it rapidly recovered from the drive its mechanical vibrations changed to electrical signals, which when amplified were displayed on the oscilloscope. When necessary the signals observed on the digital and analogue oscilloscopes were captured in the computer for later analyses as required.

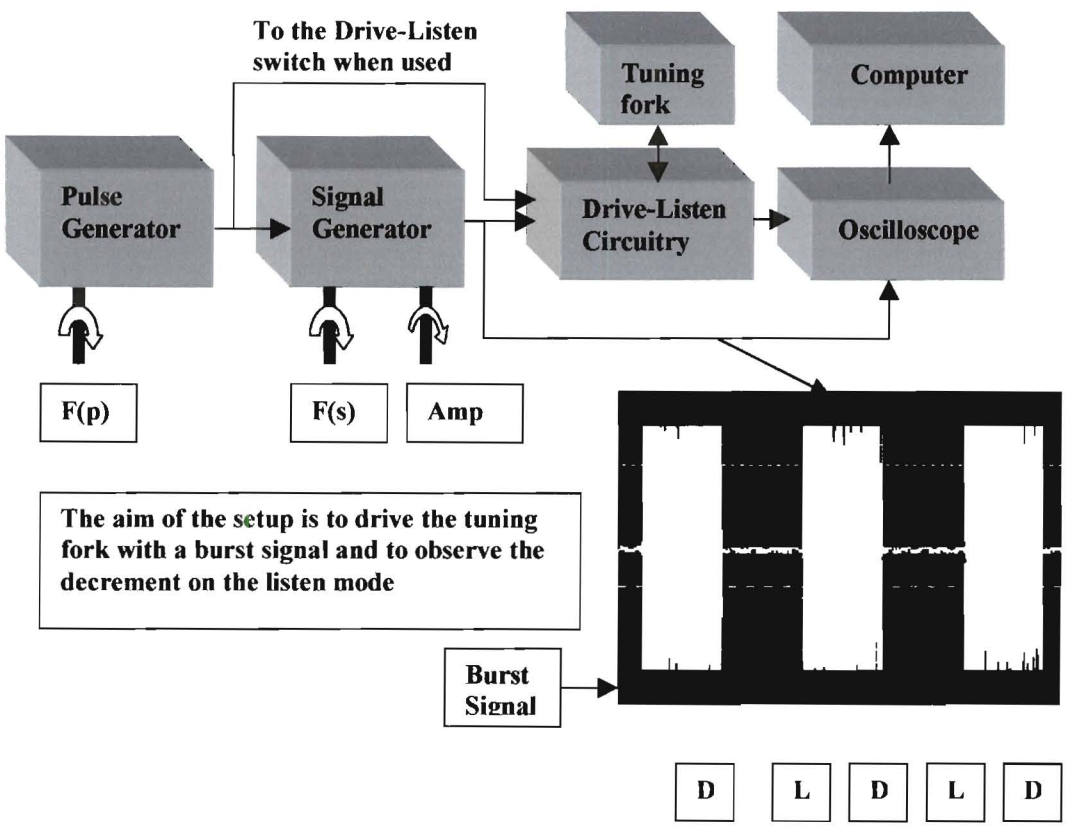

Figure 3.2: Block-diagram of the Drive-Listen signal (D and L) showing the burst signal as seen on the digital oscilloscope.

3.2 RESONANCE SETTING

Experiments were carried out using; Air, Water, Paraffin Oil and later Glycerol. Each time a run was taken, the tuning fork was set to its resonant frequency and then the decrement would be obtained on the listen mode.

To precisely set the fork to resonance, the burst signal was connected and the frequency swept through a wide range while both the amplitude and the phase of the decrement were observed. Resonance was reached when the amplitude is a maximum and was recorded on a frequency counter and the decrement on the oscilloscope. The accuracy of the frequency obtainable falls as the Q decreases.

At resonance the fork's response is at its maximum, so the signals generated by the coil are large and ensure a good signal to noise ratio. The resonant frequency of the fork is given by the equation $\delta m/M = -2\delta f/F$, therefore a fractional change in mass leads to twice the fractional change in frequency.

These operations could be automated, but the development of the necessary circuitry was not dealt with in this thesis.

3.3 MAGNETIC BIASING

For optimum performance, the fork has to be precisely biased magnetically and this is necessary as the magnetostrictive phenomenon is non linear. To get this magnetic bias right, a thickness polarised rare earth magnet was adjusted just above the coil. In the development stages, as the magnets were being adjusted a maximum output signal was picked up by the microphone when biasing was reached.

In certain cases the magnetostrictive material had sufficient magnetic retentivity for the magnets to be unnecessary, but as a precaution they were always used.

3.4 FINAL TRANSDUCER DESIGN

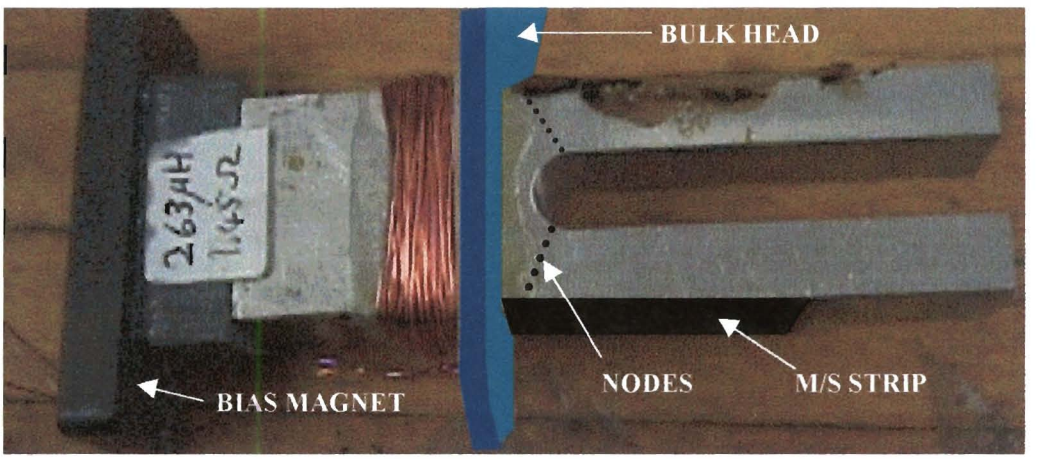

Figure 3.3: A section showing the fork interface to the liquid, with the m/s strips and their attachment to the tines. The laminations stop short of the root. The magnet was positioned to give maximum signal and the immersion of the tines can be seen.

The magnetostrictive nickel alloy strips (m/s) go through the barrier to the fork where they are held solidly flat against the tines by thermosetting arasldite. They conduct the driving AC field and the magnetic bias to the region of maximum flexure. With the alloy alone the field saturated and fell off rapidly, but much better conduction was achieved by the addition of a length of transformer lamination.

This gave a major improvement in performance, allowing the fork to have as deep an immersion into the liquids measured as possible. The improvements in electical performance were traded off against this requirement ***(gap between the tines)/(tine width*density of thefork).*** The wall seperating the electronics from the liquid gave the fork a form of a probe which made it easier for experiments to be taken.

After evaluating various forks, it was realised that the acoustic signals picked were proportional to the ratio of the ***(microphone amplitude) *(current drive)*** and Q. The magnetostrictive coupling is ***(mike amplitude)/(Q*current drive)***, and must be as large as possible.

3.5 THE PERFOMANCE OF THE FORK IS AFFECTED BY ITS GEOMETRY AND DENSITY

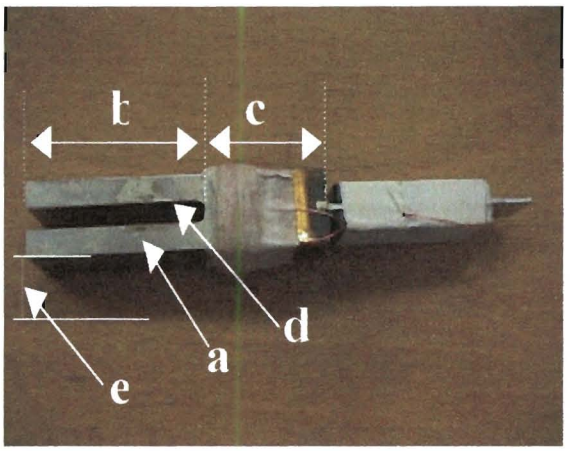

a: Tine width
b: Tine length
c: Distance from root to end of fork
d: Gap between the tines
e: Depth of tines

Figure 3.4: This diagram shows the physical dimensions of a typical tuning fork used.

Table 3.1: This table shows the physical dimensions and the various materials of the forks used.

T.F number	Material	a	b	c	d	e	Density (ρ)	e/(d*ρ)
		mm	mm	mm	mm	mm	g/cm^3	
T.F# 1	Stainless steel	6	44	33	6	25	7.9	0.030
T.F# 2	Stainless steel	8	52	37	6	22	7.9	0.035
T.F# 3	Aluminium	10	44	33	6	12	2.71	0.185
T.F# 4	Brass	10	44	34	6	26 d	8	0.029
T.F# 6	Quartz	8	49	38	8	12	2.66	0.25
T.F#8	Glass	6	59	64	7	14	2.4	0.208
T.F# 7M	Brass	8	39	9	7	7	8	0.125

Table (3.1) contains the various dimensions of the forks used, as shown by figure (3.4). The forks used include cylindrical and square designs while the materials range from quartz to stainless steel. These different forks were built and tested since it was the aim of the project to develop a dip-stick for liquid characterisation.

The sensitivity of a tuning fork depends both on its material density and its geometry, so an optimal fork design, could be developed depending on the kind of liquid to be measured and the parameter is $e/(d*\rho)$ [9].

By mass calibrating the forks, their sensitivities were obtained and could be altered by changing some few dimensions or the material as already discussed.

CHAPTER 4

DRIVE – LISTEN SYSTEM

4.1 FEARURES OF THE ELECTRONIC CIRCUITRY USED

The layout of the "Gunther" relay is shown in figure (3.2). It comes as a result of many modifications of previous prototypes that were modified as faults and problems were revealed.

The details of this circuit were left out during the last stages of the project, because of the relatively better electronic circuit that was later built. It however constitutes a large part of the project that is why it is included.

4.1.1 POWER SUPPLY

The digital part of the circuit had 5 V supply while the rest of the circuit had a variable voltage between 15 and 30 V from a variable output power supply. The voltage supply to the rails was also decoupled by 10 μF capacitors.

4.1.2 ISOLATION OF THE TUNING FORK

The tuning fork is alternatively driven and listened to as alread discussed above. During the drive cycle a large burst signal of $\pm$ 20 V_{p-p} is driven into the coil of the tuning fork. So during this phase (i.e.Drive) the circuit gives a sufficiently low output resistance to drive the low impedance tuning fork coil.

4.1.3 DRIVE CIRCUIT (see figure 4.1)

The drive circuit had a push-pull configuration. The input into the high power amplifier (LM 343) was a square wave burst signal of ± 20 V_{p-p} which had already been through a pre-amplifier circuit. The power npn and pnp transistors used, switched between ground and the supply rails before going into saturation.

4.1.4 LISTEN CIRCUIT

The listen amplifer was a current to voltage converter [21], and it had a high pass filter at its output to reduce the switching transients. In the listen mode, the tuning fork's coil could be represented as a current source. During the listen cycle, the tuning fork was directly connected to the listen amplifier and it gave significant gain for the decrement to be seen. The less inductance the coil had the larger the output signal that developed. Two clipping diodes were used to limit the output signal when the output signals were too large.

4.1.5 CONTROL AND TIMING CIRCUITRY

The drive-listen circuitry was well controlled and the relay opened and closed at precisely the right times which was necessary for the protection of the listen circuit. This ON/OFF switching of the relay was triggered by providing 25mA from a transistor to the relay's coil at pre-determined time intervals, provided by a square wave pulse from any selected output of the counter.

By combining a clock and any selected counter output signal through a NAND gate [22], the burst signal was obtained for the drive. To vary the amplitude of this burst signal, the pre-amplified signal going into the power amplifier could be controlled by a feed back potentiometer.

To set to the correct resonant frequency, the frequency of the oscillator signal from the multivibrator was altered by varying the 100k and 500k potentiometers for coarse adjustment and the 5k ten turn potentiometer for smooth adjustment.

4.2 FEATURES OF THE FINAL ELECTRONIC CIRCUIRTY

The difference between the two circuits, is how the signals were generated. With the first method the PRF and the burst were obtained from the digital circuit built while the signal and the square wave generators were used in the improved method.

4.2.1 CONTROL AND TIMING CIRCUITRY

The improved method could be used with and without the relay. Without the relay the tuning fork's coil was driven and listened to at the same point, and with the relay the coil was either connected to the drive or the listen circuit at one time.

The PRF switch on the wavetek pulse generator was altered to vary the duration of the drive-listen signal. To set the tuning fork to its resonant frequency both the coarse and the fine frequency switches on the signal generator were used.

4.2.2 DRIVE CIRCUIT

The drive circuit had no pre-amplifier, so the drive signal was connected directly on the power amplifier and its amplitude could be altered by adjusting the amplitude knob on the signal generator. The burst signal used in this case was also sinusoidal and had no harmonics.

The other parts of the drive circuit used in this system are similar to the one already discussed above. The circuits shown below are the votage and the current circuits used for driving the fork.

4.2.3 TRANSDUCER COIL

During the early stages of the project, the tuning forks used had coils wrapped around their upper part very close to the root like those in figure (2.1) and their inductance rating was between 1-3 mH. After several experiments it was then decided to reduce the inductance to between 0.2-0.5 mH. As a result a significant improvement was noticed on the decrement obtained since the total impedance of the system decreased.

By correcting the power factor of the tuning forks, more energy could be put into the actual driving of the transducer. This was achieved by connecting a capacitor of similar reactance to that of the fork's coil, but adjusted to make the input voltage a maximum at the frequency used. The transducer thus presents a parallel tuned circuit to the drive. The impedances can be 5-10 ohms and the drive amplitude can be a few volts. The emf from the coil to the listen circuit has a low source impedance. For listen a gain of more than 100 is needed, and by feeding the emf directly to the invert input of an op-amp the full listen power is used and a good signal to noise ratio is achieved. Further the minimisation of noise was obtained by using a flatly tuned circuit in the op-amp feedback.

An important practical requirement is to have a wide practical distance between the coil and the barrier allowing a more extensive immersion in the liquid.

4.2.3a VOLTAGE DRIVE CIRCUIT

The circuit gives a sufficiently low output resistance to drive the low impedance tuning fork coil. The listen circuit here was connected across the coil and it was designed to have a rapid recovery from the drive and to give the high gain required for listen. The listen signals obtained were relative to ground.

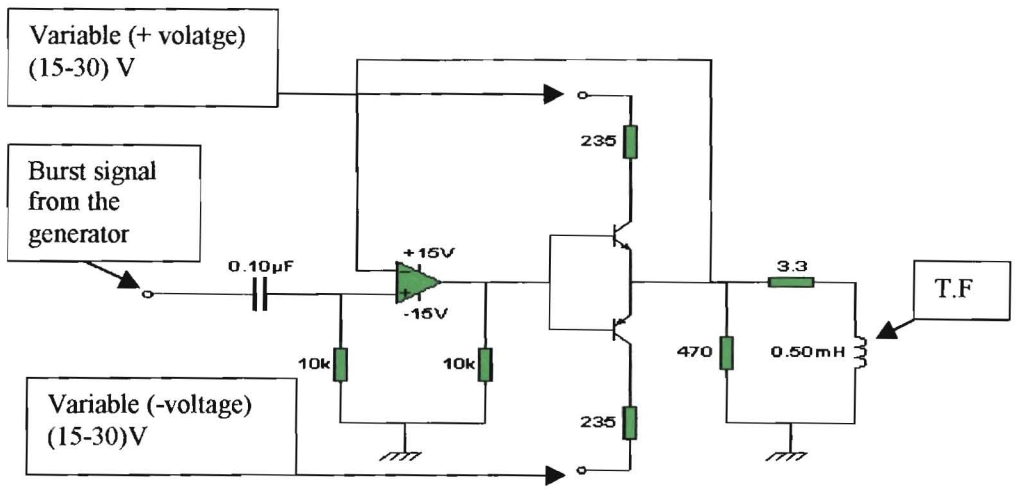

Figure 4.1: Voltage drive circuit. The low impedance load requires the low impedance drive.

4.2.3b CURRENT DRIVE (Figure 4.2)

Figure (4.2) is a convenient alternative to the voltage drive already described. In the current drive circuit there is a D.C current bias through the coil which is modulated by the burst signal. The tuning fork voltage is relative to the positive rail. An emitter driven pnp transistor amplifier makes the output relative to ground. It, like the Op-Amp circuit has the necessary fast recovery time. It is this circuit that was finally used for the liquid measurements carried out.

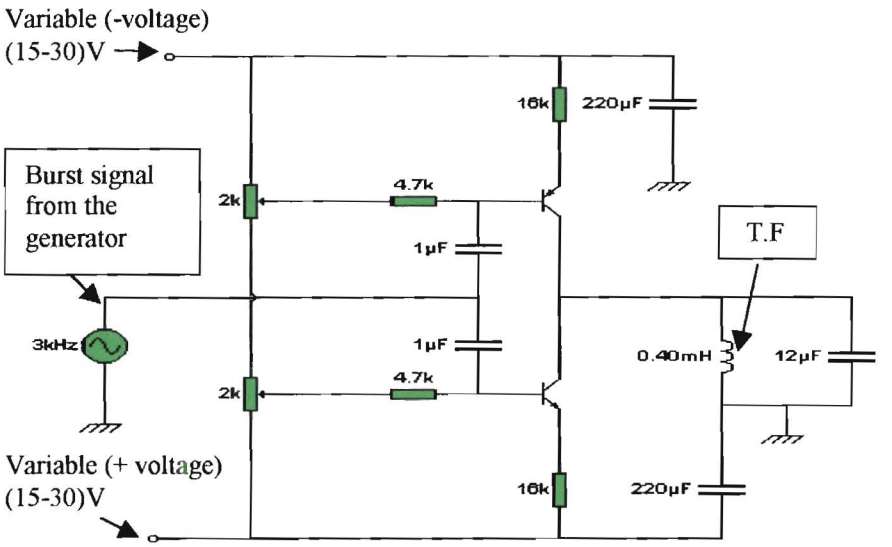

Figure 4.2: Current drive circuit. The collector gives a push pull current drive to the coil which is flatly tuned.

4.2.4 LISTEN CIRCUIT

This is the inverted amplifier of an op-amp. The input is directly from the fork and has a low source impedance of about 10Ω. By using an inverting amplifier, the full power of the listen signal is used. The current flows directly from the fork's coil to the op-amp's feedback impedance. The feeback is flatly tuned over the range needed by the particular fork. For example by connecting the 470Ω, 5mH and 0.66µF in parallel on the first amplifier, only the tuning forks with the resonant frequencies between (2.3 – 2.8) kHz were used. The tuning plus the CR filter used improved the signal to noise ratio and gave clean noise free waveforms. The output decrement is very small hence it is magnified more than 100 times by the two amplifier stages for it to be properly measured. The back to back diodes were only used to limit the output to ±0.7V when used with the storage scope, since it was found to be having a high saturation limit.

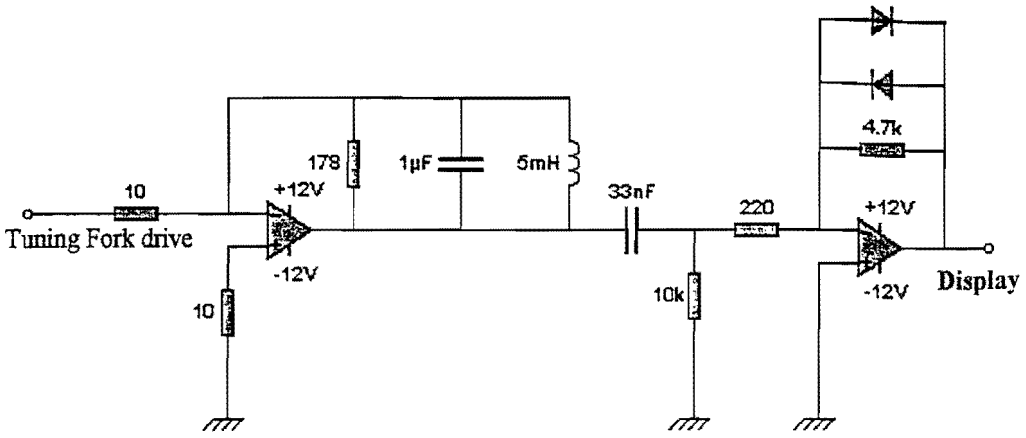

Figure 4.3: Listen circuit. The low source impedance of the unit leads to a good listen signal.

There are three selective circuits in the system. The fork which is high Q, the coil drive which is low Q and the listen circuit which has a useful selectivity. The feedback impedance of this listen circuit was found to be ±2.46k. As a result the when the forks are connected directly without the 10Ω, their gain is different since it depends on their R_o values as shown in the table below.

Table 4.1: This table shows that various forks have different gain due to their R_o values obtained using equation (2.18).

FORK	Fork #6	Fork #3	Fork #1
	QUARTZ	AL2	S.S FORKA
Vo	9	12.19	22.03
V_{10}	5.812	5.062	12.34
Ro	18	7	13
Vcoil	9.844	7.812	1.875
GAIN	137	351	189

To precisely get the value of the back emf when using various forks, the amplified output signals obtained were divided by the required gain.

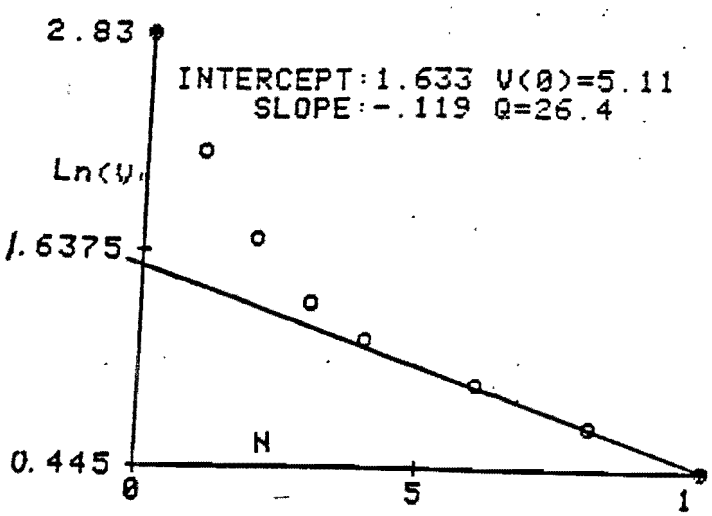

Figure 4.4 The switching transient causes false readings in the early part of the "log-dec".

CHAPTER 5

MERSUREMENTS CARRIED OUT IN THE PROJECT

The first experiment carried out was to drive the fork with a burst signal and to observe its relationship to the decrement signal on the listen cycle.

The second experiment carried out was to establish the effect of both the mass and the loss loading on a vibrating tuning fork. This was achieved by driving the fork in different lossy liquids like (Water , Paraffin and a standard car Oil) and the results were referenced to the air results obtained.

The third experiment was a mass calibration of the various forks so as to get their sensitivities. Mass calibration of these various forks was carried out by attaching additional weights to the tuning fork's tines whilst observing their effect on frequency.

The fourth experiment was to evaluate the coupling efficiency of various forks in liquids, and to characterise the liquids based on their density and thickness.

The firth experiment was carried out to show how the liquid's properties vary with temperature. This was done by heating and cooling oil and glycerol between 2°C to about 60°C while stirring during the heating process so as to evenly distribute the heat. For heating, a hand held electric element was used while dry ice, liquid nitrogen and ice cubes were used for the cooling process.

Tuning forks detailed in table (3.1) were used throughout the experiment. Their effectiveness for various applications were evaluated.

5.1 TESTING OF THE DRIVE-LISTEN SYSTEM.

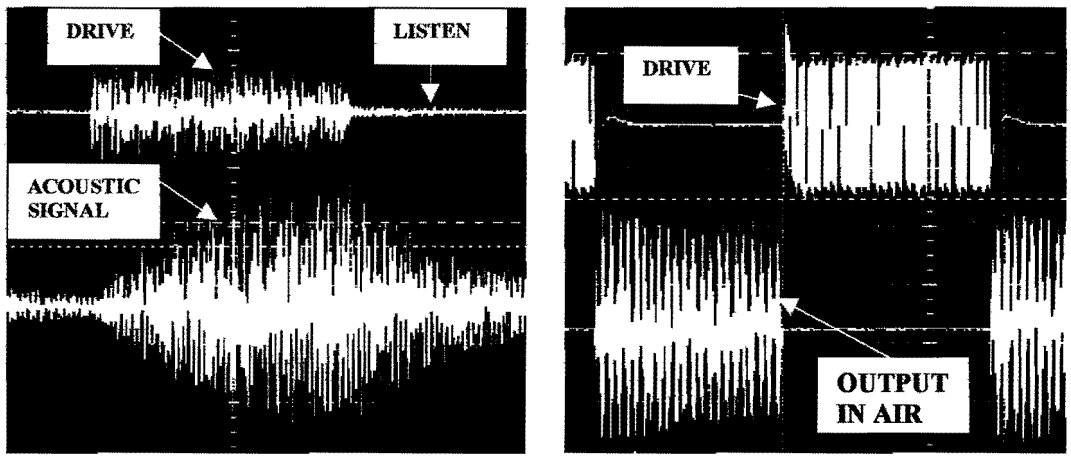

Figure 5.1: The diagram shows the acoustic signal and the output decrement on the listen phase. The drive signal can be up to 40V and the listen signal as lows 2mV(86 dB).

During the drive cycle the fork is driven by a high power burst signal and the PRF is selected such that the maximum drive is put into driving the tuning fork. By using an acoustic signal displayed in figure (5.1) above, it is seen that the conversion of electrical energy to mechanical is minimum at the start of the burst and approaches maximum towards the end of the burst. In thick liquids both the acoustic and the listen decrement are much smaller because of the extra loading that the fork experiences. This loading phenomenon is shown below where the fork is driven in different liquids.

On the listen phase the mechanical vibrations of the fork are converted to electrical signals, and are at maximum at the start of the listen phase and gradually decrease until the next drive cycle starts. This decrement obtained on the listen cycle is the one used in the liquid's loss loading measurements. The decrements on the listen phase are many times smaller than the drive signal, so they have been amplified by more than 100 times to be properly analysed.

5.2 LOADING EFFECTS ON A VIBRATING TRANSDUCER

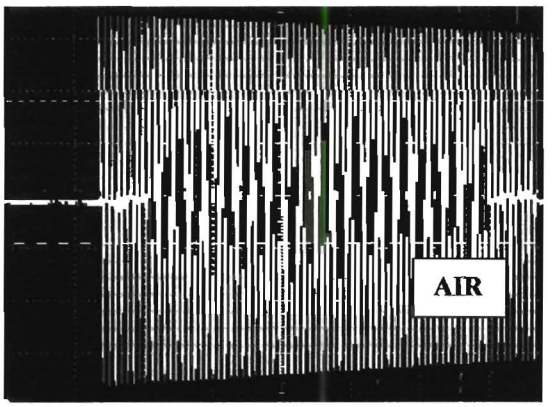

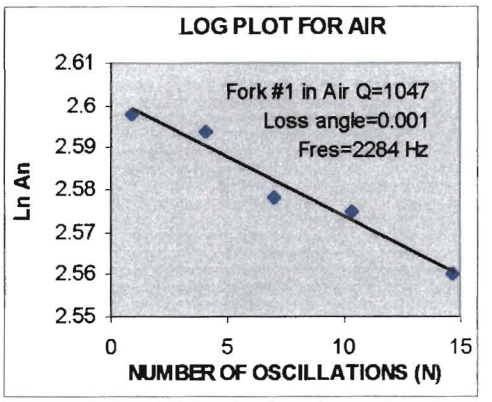

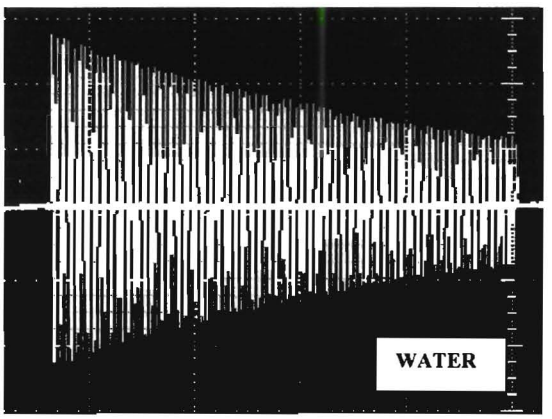

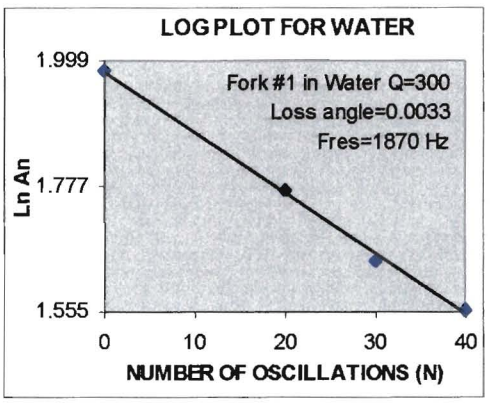

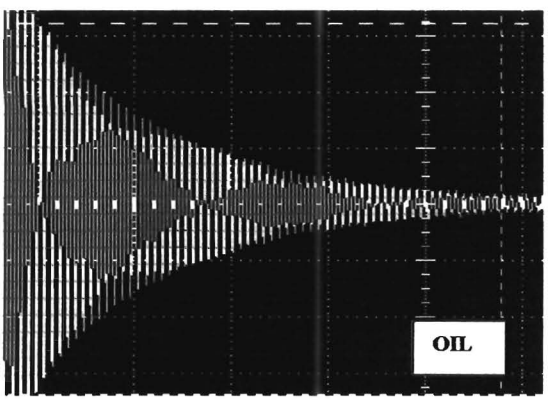

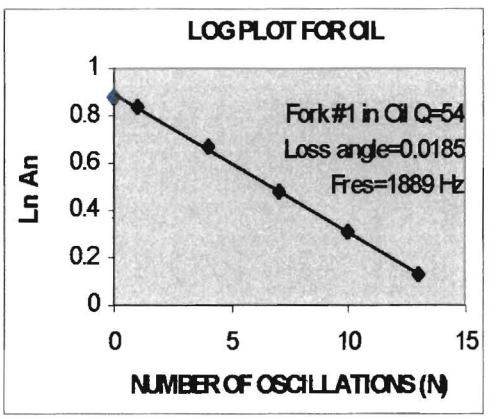

Figure 5.2:The decrement falls fast in a thick oil compared to when in water and air. The graphs show the slope of the waveforms from which Q is calculated. N represents the number of oscillations.

Table 5.1: The fall in frequency for water is greater than the fall for oil since water has a greater density. The loss however is greater for the thick oil.

FLUID	F(Hz)	Chnge in F (Hz)	%F	Q	1/Q
FORK #1					
AIR	2284	0	0	1047	0.00096
WATER	1870	414	18.1	300	0.00333
OIL	1889	395	17.3	54	0.01852

The data in table (5.1) and figure (5.2) above was obtained by driving Fork #1, a stainless-steel tuning fork in Air, water and Oil. The listen signals obtained are in a form of a decrement, where a very sharp fall resulted for oil as compared to water whilst taking the air results as a reference. The rate of fall, which is the slope of the decrement is inversely proportional to Q of the system as shown in table (5.1). When driven in air the only losses experienced are the internal losses of the fork and when in liquids there are extra losses due to the liquid's density and viscosity.

According to table (5.1) the fork operating in oil has the lowest Q of 54 compared to water and air at 300 and 1047respectively. The inverse of Q (the loss angle) is therefore highest in oil meaning that the fork vibrating oil is more heavily damped than when in water and air. As a result the fork's vibrations die quicker as shown by a very sharp decrement in figure (5.2) above.

The resonant frequency of the fork depends on the liquid under examination, and it was found to have fallen by (18.1%) in water and by only (17.3%) in oil.

By analyses it is seen that the higher frequency drop in water is due to its higher density whilst the higher energy loss in thick oil is due to its higher thickness leading to greater internal losses. In case of oil there is also inertia due to the sticking and dragging of oil on the tuning fork. From these results it is clear that a tuning fork can be used to monitor the fluid's loss loading and mass loading. It is to be noticed that the term "viscosity" only applies strictly to "simple" liquids.

5.3 MASS CALIBRATION OF VARIOUS TRANSDUCERS

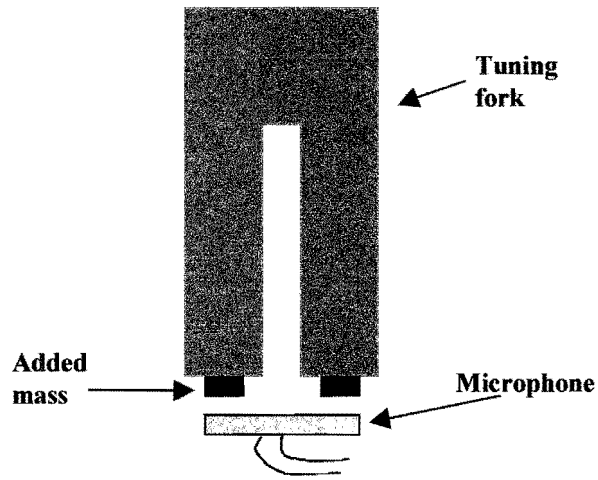

Figure 5.3: This diagram shows the setup used for mass calibration of various transducers. The acoustic signal was used to compare the efficiency of these transducers during the development stages.

In this experiment two nuts of 0.64g each were glued to the tines to provide the extra known mass loading necessary for the calibration of various forks. The frequency changes of each fork with and without the added mass were used with equation (2.3) to find the fork's equivalent mass and sensitivity. The sensitivities of some of the forks used are listed in table (5.2) below.

The results obtained with and without the nuts, show that the lumped equivalent mass is very low in light forks made of quartz and aluminium when compared to the heavier brass and stainless steel forks used. Therefore, these light forks have a higher sensitivity compared to the heavier ones, and this is shown by the data for fork #6 (Quartz) and fork #3 (Aluminium) against fork #1 (stainless steel) and fork #7 (brass) forks.

Table 5.2: The sensitivity of the various forks used was obtained by mass calibration. Fi is the frequency measured without the added mass, whereas Fm is that with the added mass.

FORK no:	Initial freq (Fi)	freq with Mass (Fm)	Fi-Fm	Mass	Sensitivity
	Hz	Hz	Hz (ΔF)	g (Δm)	ΔF/Δm (Hz/g)
1	2283.8	2222.2	61.6	23.7	2.600
2	1511.2	1485.5	25.7	37.6	0.684
3	2899.7	2655.2	244.5	7.6	32.000
4	2905.5	2851.3	54.2	34.3	1.580
5	2755.2	2704.5	50.7	34.8	1.457
6	3063	2780	283	6.9	41.000
7	1422.4	1398.5	23.9	38.9	0.627

By comparing fork #1 and fork #3, it is seen that fork #3 has a much higher sensitivity than fork #1 despite their similar geometry. So by choosing a low-density material for the fork increases the sensitivity for any geometrical design. The sensitivity of the two forks fork#1 and fork#2 having the same materials was also found to differ, thus confirming that the sensitivity of the fork also depends on its geometry.

To vary the sensitivity of the transducer, the geometry can be altered by either increasing or reducing the gap between the tines (d), by reducing the thickness of the tine (a) or by increasing the tine's (e) depth. The length of the tines (b) does not have much effect on the sensitivity of the fork, so the fork's size could be reduced by shortening the tines.

5.4 TRANSDUCERS ENERGY CONVERSION FROM ELECTRICAL – MECHANICAL.

Another way of classifying transducers is by evaluating their energy conversion from electrical to mechanical, by taking the ratio of their drive to the listen signal and their loss angles. The best fork is the one with the biggest listen signal hence the lowest drive to listen ratio and the lowest loss angle. The listen signal is very low, so it was amplified by more than 100 depending on the Ro of the fork used, for measurement to be accurately taken.

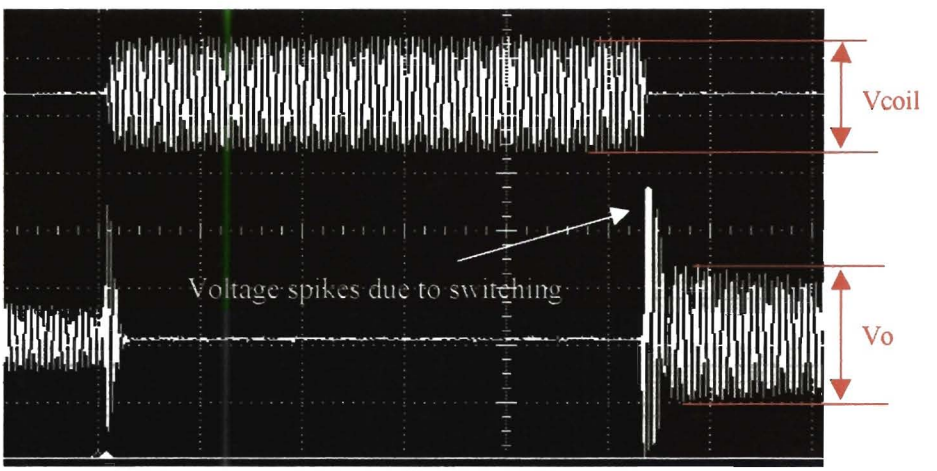

Figure 5.4: The drive voltage V_{coil} is obtained from the burst signal and the amplified listen signal V_o is the maximum signal of the decrement.

This experiment was carried out to evaluate the forks's efficiencies. Various tuning forks were driven in air, water, paraffin, oil and glycerol and the ratios of their coil voltage against the listen signals were calculated and compared in the table (5.3).

The switching transients at the beginning of the listen signals shown in figure (5.4) intrude on the first cycles of the decrement, so a careful measurement was taken when measuring the decrement voltage (V_o). The drive voltage was measured across the coil and is shown in the table as V_{coil}. The loss angles obtained using different forks in a range of liquids were also obtained and compared with the ratio of V_{coil}/V_o.

Table 5.3: This table shows the relationship of V_{coil}/V_o as plotted against the loss angle (1/Q) for various forks operating freely in air. The losses in air are due to the internal losses of the forks.

FORKS	Also called	Vcoil	Vo	Vcoil/Vo	Q	Loss angle (1/Q)
		V	V			
Fork #6	Quartz	3.063	18.69	0.164	757	0.001321
Fork #1	S.Steel	0.281	12.59	0.022	1047	0.000955
Fork #3	AL2	6.375	8.625	0.739	142	0.007042
Fork #5	S.Steel cyl	3.672	5.539	0.663	740	0.001351

The data shown above was obtained with the transducers operating freely in air with no external loading. Shown in the table fork #1 has the highest Q compared to the other forks used. Fork #6 and fork #5 have the next highest Q values respectively, with fork #3 having the lowest Q.

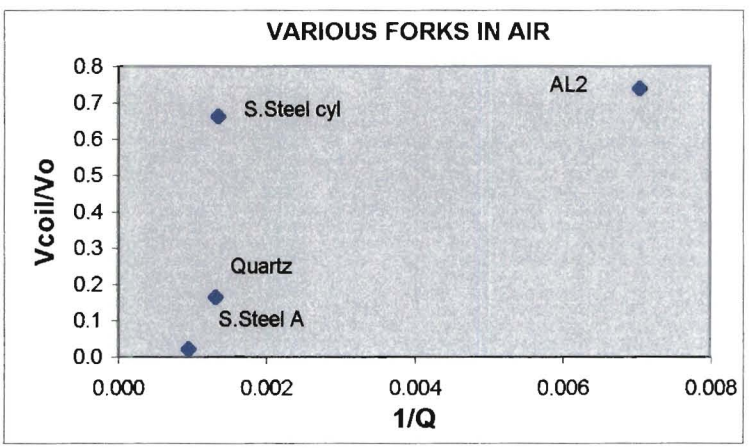

Figure 5.5: This graph shows V_{coil}/V_o plotted against the loss (1/Q). The best transducer from these results is S.Steel A with the lowest loss angle and the lowest V_{coil}/V_o.

S.Steel A and Quartz have the lowest V_{coil}/V_o ratios due to their relatively high coupling co-efficients when compared to the other two forks. Due to their high coupling co-efficients, they have the best energy conversion from electrical↔mechanical, shown by their high listen output V_o. These forks also have the lowest loss angles, probably due to their very low internal resistance.

The results obtained here can be taken as a reference to evaluate the perfomance of these forks in liquids where evidently different liquids add extra loading to the transducers used.

5.5 EVALUATION OF HIGH AND LOW SENSITIVITY TRANSDUCERS IN LIQUIDS

In this experiment , a range of liquids namely water, paraffin, oil and glycerol were measured using different forks. Due to different sesitivities of the forks used, there are differences in Q factors and the frequencies obtained. Below there are three tables of data obtained when using a low sensitive fork (Fork #1) and the two high sensitive forks (Fork #3 and Fork #6). The percentage drop in frequency and Q are shown with reference to the results.

Table 5.4: A low sensitive fork (fork #1) was driven in various liquids (water, paraffin, engine oil and glycerol) and due to its good coupling good measurements were obtained in very thick liquids.

FORK #1	AIR	WATER	PARAFFIN	ENGINE OIL	GLYCEROL
S.Steel A					
Vcoil	0.281	0.47	0.613	0.650	0.7
Vo	12.59	8.75	0.375	2.422	1.238
Frequency	2284	1870 (18.1%)	1935 (15.3%)	1889 (17.3%)	1777 (22.2%)
Vcoil/Vo	0.022	0.054	0.065	0.268	0.565
Q	1054	303 (71%)	422 (60%)	54 (95%)	28 (97%)
1/Q	0.0009	0.0033	0.0024	0.0185	0.0357

Table 5.5: A high sensitive fork (fork #6) was driven in various liquids (water, paraffin, engine oil and glycerol) and it also has a good coupling enabling the transducer to be used for measurements in thick liquids.

FORK #6	AIR	WATER	PARAFFIN	ENGINE OIL	GLYCEROL
Quartz					
Vcoil	3.063	3.375	3	9.844	3.406
Vo	18.69	10.38	17	9	4.906
Frequency	3109	2362 (24%)	2477 (20%)	2397 (23%)	2227 (28%)
Vcoil/Vo	0.164	0.325	0.176	1.094	0.694
Q	757	319 (58%)	330 (56%)	34 (95)	28 (96%)
1/Q	0.0013	0.00313	0.00303	0.02941	0.03571

Table 5.6: A high sensitive fork (fork #3) was driven in various liquids (water, paraffin, engine oil and glycerol) and it also has a good coupling enabling the transducer to be used for measurements in thick liquids.

FORK #3	AIR	WATER	PARAFFIN	ENGINE OIL	GLYCEROL
AL 2					
Vcoil	8.563	7.44	7.81	7.44	7.06
Vo	16.5	13.9	12.2	5.5	4.719
Frequency	2885	2241 (22%)	2344 (19%)	2294 (20%)	2119 (27%)
Vcoil/Vo	0.520	0.535	0.64	1.353	1.496
Q	142	117 (18%)	122 (14%)	31 (78%)	21 (85%)
1/Q	0.0070	0.0085	0.0082	0.0323	0.0476

When forks operate in liquids they do not vibrate freely as they do in the air, infact they experienced additional load due to the mass and the loss loading of the liquids. The greater the density and the thicker the liquid is, the greater is the total loading induced on the fork. As a result of the increased loading , (V_o) the output voltage becomes smaller at the start of the listen signal followed by the decrease in frequency and the increase in the loss angle(I/Q).

The percentage drop in the Q values and the frequency is the highest for glycerol in all three tables above, therefore it confirms that glycerol is the heaviest and thickest liquid used. The liquid with the next highest drop in Q is engine oil followed by water and lastly paraffin. These results confirm that oil is thinner than glycerol but thicker than water, and that paraffin is the thinnest.

The drop in frequency is lowest in paraffin followed by oil, water and glycerol respectively, thus confirming that glycerol is heavier than all the other liquids measured, followed by water, oil and lastly paraffin.

When calibrated the frequency gives the liquid density and the loss angle gives the liquid's viscosity.

The frequency drop in these the liquids is larger when using the more sensitive forks (fork #6 and fork #3). The change in Q for the different liquids above is however more noticeable when using a less sensitive fork (fork #1). The results therefore show that tuning forks with high sensitivity couple strongly with the liquid, whereas forks with low sensitivity have very low coupling to the liquid. Hence a low sensitive fork (fork #1) is better for the general measurements of the very thick liquids whereas more sensitive forks (fork #3 and fork #6) would be better for use in simple thin liquids.

5.6 DAMPING OF THE FORKS VIBRATIONS IN LIQUIDS IS DUE TO BOTH THE LIQUID'S DENSITY AND VISCOSITY

The graphs of the drive divided by the listen output (V_{coil}/V_o) against the loss angle (1/Q) are displayed to show the effect of both the mass and the loss loading on the vibrations of the forks.

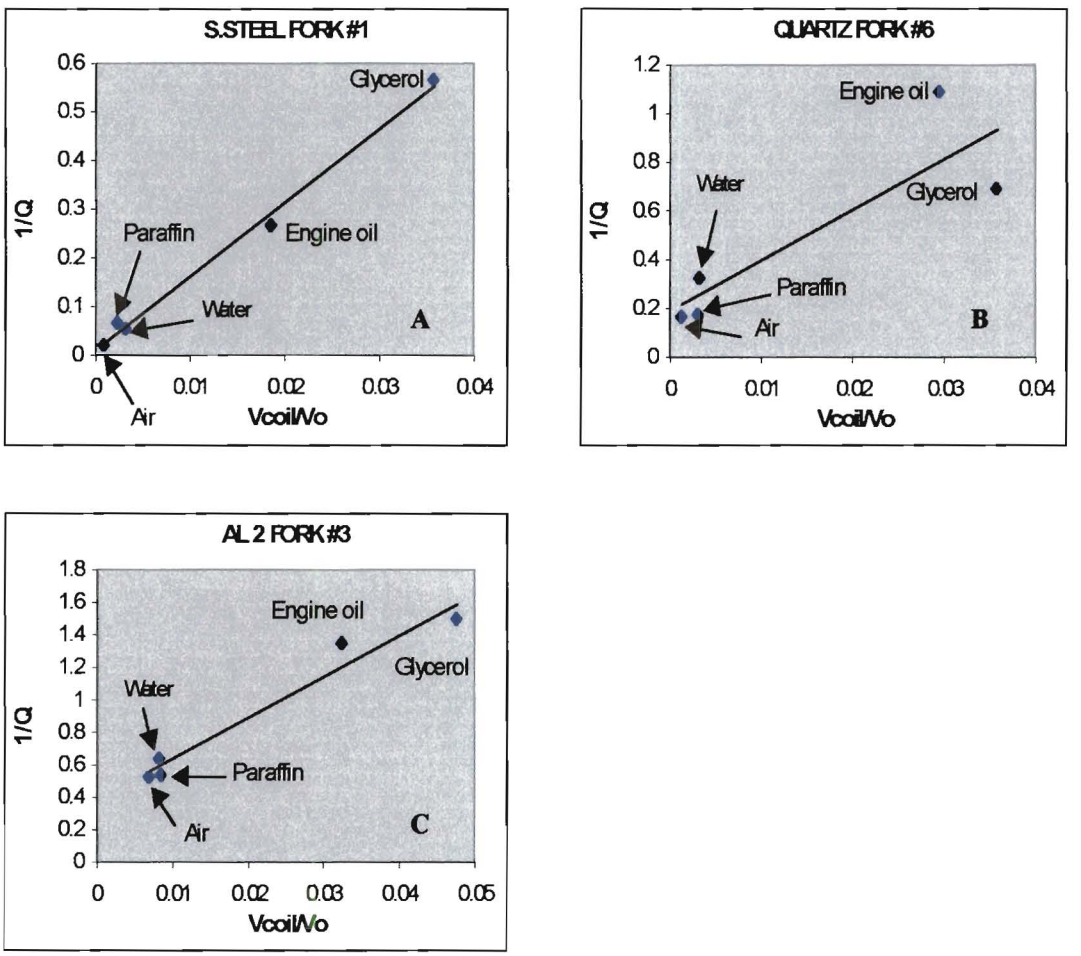

Figure 5.6: An overview of the transducer perfomances.

The three graphs above show that the output signals continuously become smaller as the loading increases. This then makes the ratio of the drive to the output larger as shown in the graphs. The square of the slope, of the ratio of the reciprocal of the output to the drive plotted against the loss angle give the coupling efficiency.

The points on the graph marked (A) above are almost linear, starting from air, paraffin, water, engine oil and glycerol. These results show that the loss angle increases linearly with the increase in thickness of the liquid. These graphs show that glycerol has the highest loss angle, and that the amplitude of vibrations in it are smaller and decay faster than in other liquids. In thinner liquids the liquids the amplitude of vibrations are larger and the duration is longer.

When using a very light sensitive fork (Fork #3), there is some incosistency, causing the points to be scattered on the plot. Some points are shown with loss angle at its highest value with its corresponding output voltage shown in graph (B). This behavior is likely due to sticking and dragging of the light fork on the thick liquids.

The coupling efficiency of the stainless steel fork (Fork #1) is higher than that for the two other forks used, hence better results were obtained. Therefore when using a heavy stainless steel fork (Fork #1) the inconsistency in the measurements when using thick liquids was avoided.

5.6.1 RESONANT FREQUENCY DROPS AS THE LOADING INCREASES

The two graphs shown by figure (5.7) below, show the decrease in frequency as the loss angle increases from air to glycerol. These graphs show that glycerol has the highest frequency decrease, followed by water, oil and paraffin respectively. A high sensitivity fork (Fork#6) shows a high sensitivity to frequency each time a different liquid is measured, and this makes it a better choice for density measurements in thick liquids. A low sensitivity transducer (fork#1) gives better overall results compared to all the other forks used, therefore making it a good general instrument for both the density and viscosity measurements.

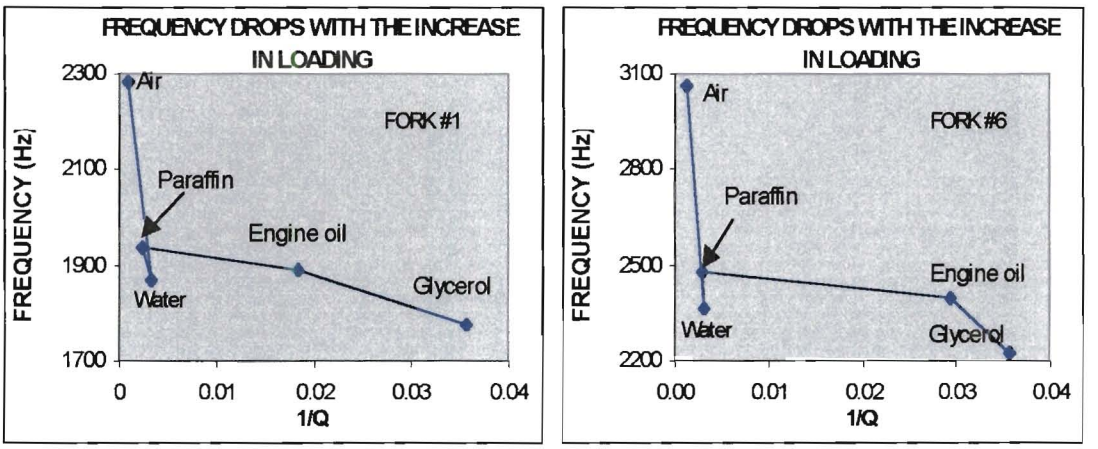

Figure 5.7: The frequency decrease is high when measuring high density liquids.

5.6.2 THE LOSS LOADING IS INVERSELY PROPORTIONAL TO TEMPERATURE IN THICK LIQUIDS

When the fork is immersed in a liquid the tines pump the liquid, thus absorbing the energy and causing a mass loading. The former, a loss that damps the vibrations, lowers the Q and the decrement in the drive-listen mode. From each of these two parameters the loss angle of the liquid can be found.

The inertial loading produces a fall in frequency from which the density can be obtained. In simple thin liquids the loss angle and density describe dynamic behavior completely. For complex thick liquids these parameters can vary with frequency and temperature.

In general the loss angle falls with the rise in temperature and shows itself in the increase in Q. The aim of this experiment is to confirm that the increase in temperature lowers the loss angle of thick liquids. In this section a series of experiments were carried out in both cold and hot oil and hot and cold glycerol. To increase the temperature of the liquids a small hand held heater was used, and the temperature range of the experiment was between 2°C and 60°C. The heat was evenly distributed by stirring the liquids thoroughly before each run, while the experimental setup remained constant.

The waveforms below were obtained in hot oil experiment. The waveforms of other liquids at different temperatures follow the same pattern as the ones shown below.

The waveforms below were obtained using fork #1 at four different temperature points (i.e. at room temperature 25^0C, 38^0C, 43^0C, and at 54^0C). At room temperature the output signal dies out fast and as the temperature rises the decrement starts to have larger amplitudes which last longer.

5.7 OIL MEASUREMENTS

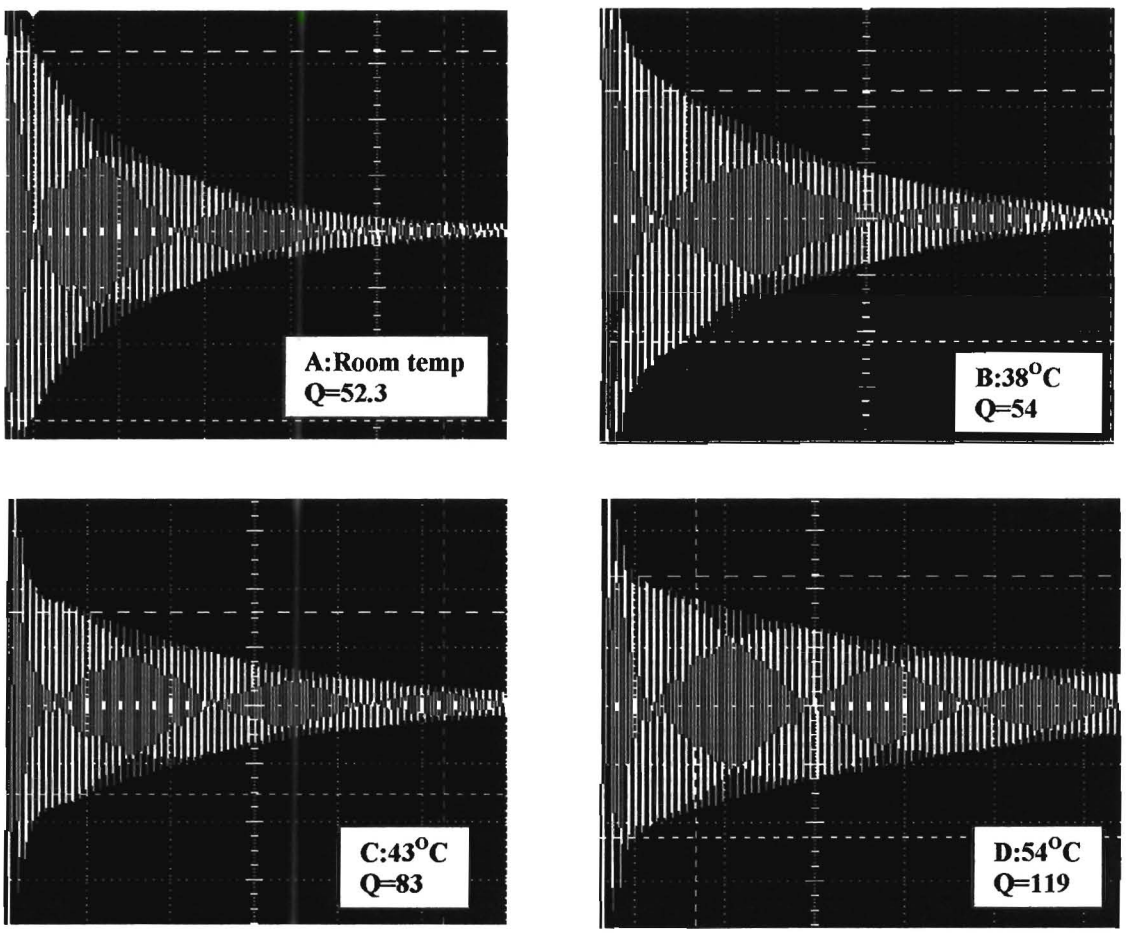

Figure 5.8: Decrements obtained for oil heated from room temeprature to 54°C. At higher temperatures the decay is slower than at lower temperatures.

The logarithmic plots drawn, show the decrease in slope as the temperature increase.

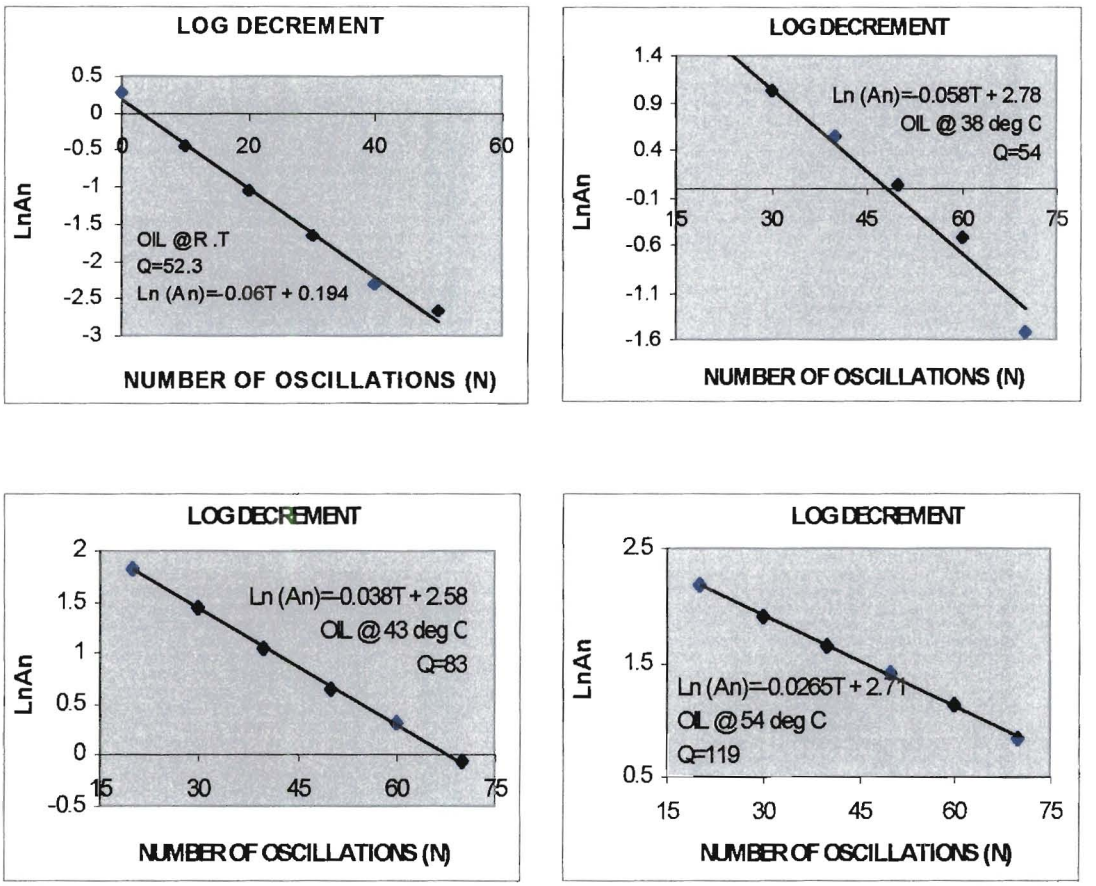

Figure 5.9: The logarithmic plots drawn show the decrease in slope as the temperature increases. The Q factor obtained is equal to π/slope.

The log plots show that the measurements were accurately taken. By comparing the decrement and the log plots given, it is seen that at 54^0C the decrement obtained decays much slower than at room temperature. The higher slope at R.T and the smaller one at 54^0C confirm that the increase in temperature makes the oil thinner and enables the vibrations to become larger and last longer. As a result the loss angle is reduced proving that a temperature increase reduces the viscosity of oil.

This experiment thus proves that the fork can detect the decrease in the liquid's thickness as the temperature rises. It can therefore be used for the classification of liquids based on their viscosities.

The data about two other forks (fork #6 and fork #7)driven in oil is laid out in the tables below.

Table 5.7: A high sensitive quartz fork (fork #6) driven in hot oil.

FORK #6 IN HOT OIL					
QUARTZ					
TEMP (^{O}C)	23	41	47	50	56
Frequency	2328	2377	2366	2362	2360
Q	30	42	48	53	54
1/Q	0.0333	0.0240	0.0208	0.0189	0.0185

Table 5.8: A low sensitive brass fork (fork #7) in hot oil.

FORK #7 IN HOT OIL				
BRASS				
TEMP (^{O}C)	23	38	43	56
Frequency	1232	1235	1235	1235
Q	53	54	83	119
1/Q	0.0189	0.0185	0.012	0.0084

5.8 GLYCEROL MEASUREMENTS

The procedure for the measurements in glycerol is the same as in hot oil.

Table 5.9: The data for fork#3 driven in cold glycerol is displayed below.

FORK #3 IN COLD GLYCEROL						
AL 2						
TEMP (^{O}C)	5.5	11.5	14.5	19.8	20.1	25.9
Frequency	2101.5	2116	2118	2111	2111	2111
Q	16	17	19	19	19	24
1/Q	0.0625	0.0558	0.0556	0.0538	0.0529	0.0417

The results of the experiments in glycerol and oil are shown in tables (5.7, 5.8 and 5.9) and they were obtained while using forks #(3, 6 and 7) at varying temperatures. A fork with very high sensitivity was driven in glycerol with the temperature ranging between 5.5^0C and 25.9^0C. At very low temperatures, glycerol is very thick hence the loss loading is too large. This is shown with a small Q value at low temperature and a steadily increasing Q as the temperature rises.

Table 5.10: The data for fork #1 driven in glycerol is displayed below

FORK #1 IN GLYCEROL					
S.STEEL A					
TEMP (^{0}C)	10.5	38.5	7.5	7	24.5
V_O	14.19	21.06	12.31	10.41	16.3
V_{coil}	11	6.437	11	11	6.44
V_O/V_{coil}	1.290	3.272	1.119	0.946	2.531
Frequency	1773	1776	1770	1766	1776
Q	25.9	51	23.6	21	37.4
1/Q	0.039	0.020	0.042	0.048	0.027

To get the data in the table above, fork #1 was driven in glycerol with the temperature ranging from 7^0C to 39^0C. The aim was to check if fork #1 could be used in very thick liquids.

The low sensitive foks (fork #1 and fork #7) have higher Q values compared to the low sensitive forks when used in thick liquids.

5.8.1 TRANSDUCER VIBRATIONS INCREASE WITH AN INCREASE IN TEMPERATURE

As the temperature of glycerol increases it becomes increasingly thinner making it easier for the fork to vibrate in it. From the graph below V_0 is seen to be increasing by a factor of 0.074 per ^{0}C increase in temperature as the internal losses in glycerol decrease.

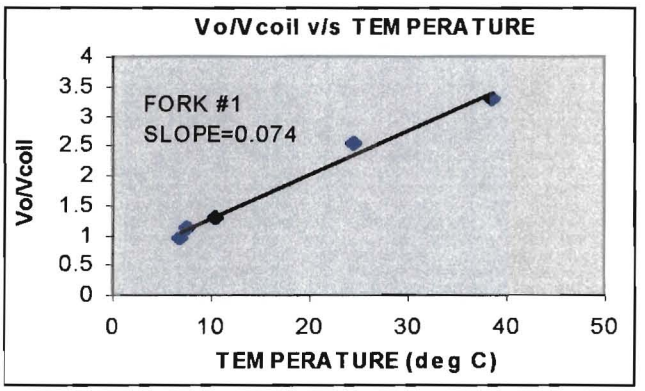

Figure 5.10: The output voltage increases as the temperature of glycerol rises

As glycerol becomes thinner with an increase in temperature, the vibrations of the fork become larger and last longer due to the decrease of about 0.0008 in loss for each ^{0}C increase in temperature.

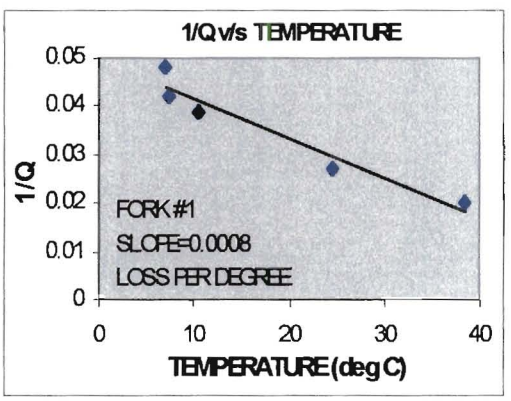

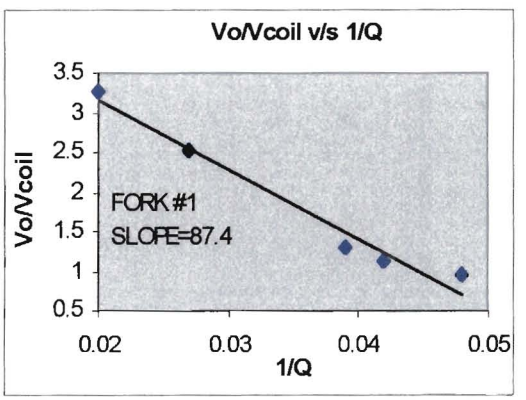

Figure 5.11: The loss angle decreases by about 0.0008 per ^{0}C increase in temperature. As the liquid becomes thinner the vibrations become larger and last longer.

As the temperature continues to rise, glycerol becomes even thinner up to a point where the temperature increase no longer affects its thickness thus allowing the transducer vibrations to increase by a factor of a about 87.74 for each °C increase in temperature.

The plot in figure (5.12) below was obtained while driving fork #3 in glycerol from 5^0C to about 30^0C. The loss per degree increase in temperature is 0.0009.

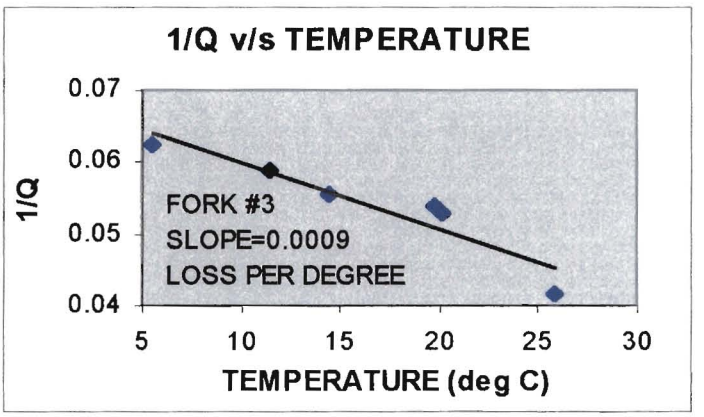

Figure 5.12: The loss in glycerol with a light sensitive aluminium fork decreases by about 0.0009 per ^{0}C increase in temperature.

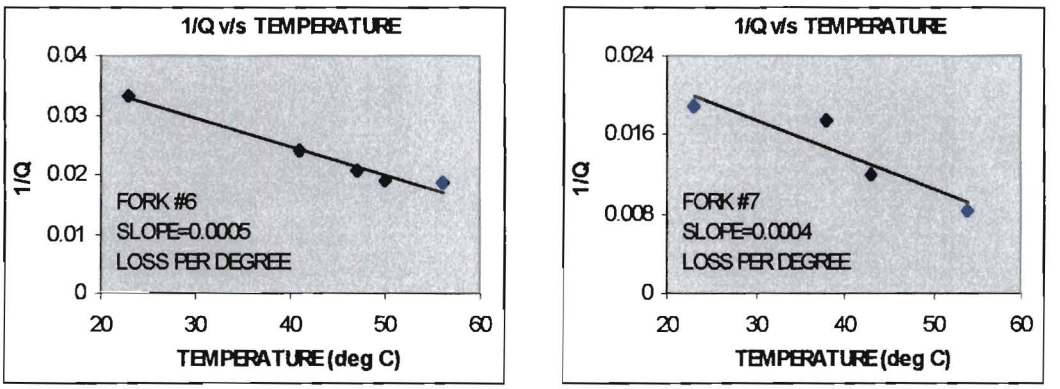

Figure 5.13: The loss angle decreases as the temperature increases. The loss per ^{0}C is more in a light fork (fork #6) than in a heavy fork (fork #7).

The loss angle of a fork represents all the losses in the system, viscous, acoustic and internal friction of the transducer material. As the temperature increases the loading on the transducer is due only to the density of oil. Therefore the decrease in the loss angle can be taken as a measure of the liquid's density.

5.8.2 FREQUENCY CHANGES DUE TO TEMPERATURE

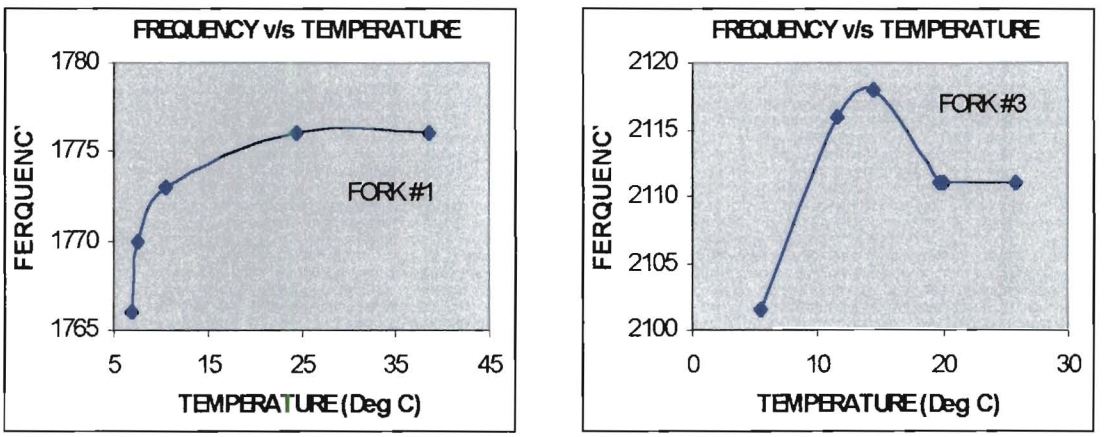

Figure 5.14: The resonant frequency of a heavy fork (fork#1) stabilises faster than that of a light fork (fork#3) when driven in glycerol at low temperatures.

When using fork #1 at temperatures between 5 and 15^0C the frequency increased by about 8Hz and by about 12 Hz for fork #3. As the temperature increase from 25^0C 45^0C the frequency remains constant.

The two other graphs shown below were obtained while driving a light fork (fork#6) and a heavier brass fork (fork#7) in engine oil.

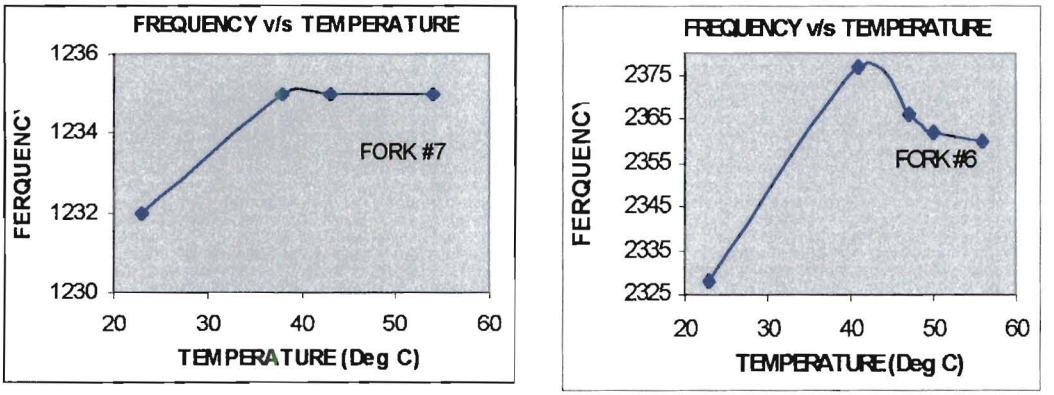

Figure 5.15: The resonant frequency stabilises faster with a heavier fork (fork #7) than with a light quartz fork (fork #6)

The forks used here were brass which being heavy has a low sensitivity and quartz, which has a high sensitivity. As the temperature rises the oil becomes conspicuously thinner with a small density change. This shows up in both cases as a rapid increase in frequency to about 40^0C followed by a constant value to 60^0C. The frequency change $\delta F/F$ for quartz is 1.4% but only 0.3%for brass in oil.

It is therefore considered that when the oil is thick there is large viscous drag adding to mass of the system but this disappears as the oil becomes thinner. At higher frequencies the loading is due to density only. As a result there is a 44% drop in the loss angle from the frequency of 2328Hz to 2360Hz for the quartz fork and 55% for the brass fork as already described in section 5.1.4.

CHAPTER6

CONCLUSIONS

Based on the results of this project, the following conclusions may be drawn:

The magnetostictive drive was used rather than the piezoelectrical drive, and was very effective in isolating completely the electrical and the vibrating parts of the transducer.

A range of transducers have been developed for suitable characterisation (density and viscosity) of a wide range of viscid liquids, particularly commercial oils and also simple liquids, where the loss factor is due to viscosity.

The transducers in the form of a tuning fork are immersed in the liquid, while the fall in the resonant frequency due to the loading and the loss given by the loss angle are measured. The loss angle has a strong dependence on viscosity, while the shift in the resonant frequency arises from the density loading.

The main challenge was to obtain measurements in very thick liquids and thus was achieved by various aspects of the design. For example heavy transducers with low geometrical sensitivity were required for the heaviest liquids. The drive was produced magnetostrictively and the actual measurements by square wave modulating the drive signal. For a 2kHz signal the modulating frequency was 20Hz giving a 100 cycle burst. The resonant frequency was then obtained from the frequency counter and the loss from the decrement when the drive is switched off. The coupling efficiency of the fork was better when the magnetostrictive strips reached further down the tine length.

The lumped mass and the internal friction of the transducer are functions of its geometry. By keeping the gap between the tines constant, and increasing the width of the fork with the same material, the sensitivity increases.

So for a given geometry the sensitivity to both parameters is inversely proportional to the fork's density.

As a result, a stainless steel fork (fork #1) due to its lower sensitivity gave good results in heavy liquid measurements, compared to the high sensitivity forks (fork #3) which is made of aluminium and the fused quartz fork referred to as (fork #6).

Finally the main objective of the project was achieved, where an instrument for general industrial use was developed. It is extremely robust and can be used in the form of a hand held "dip stick". A single screaned lead connects the unit to the electronics, which is completely isolated from the liquid by the bulkhead, therefore exluding any possibility of an electrical harzard.

Measurements have been made on a wide range of liquids and the results obtained have good reproduceability. The heaviest liquid measured is glycerol at $2^{o}C$. It is visualised that users will calibrate the individual units using thick liquids of their choice, and when suitably calibrated the transducer can be used to measure the proportions of the liquid mixtures.

CHAPTER7

RECOMMENDATIONS

From the results obtained and the conclusions drawn, it is recommended that since a complete range of transducers has been produced, they now need to be automated to:

- Hold the resonant frequency of the tranducers as the liquid properties change.
- Provide a readout of Q, for the loss angle measurements.

The automation of the system is expected to be straightforward and a simple reliable design is expected.

A number of displays have been considered. Numerical information could use a display on a cell phone type unit. An acoustic display signal could relate the pulse recurrence to the loss, increasing as the liquid gets thicker.

BIBLIOGRAPHY

1. R.D Ford, Introduction to acoustics, Elsevier Publishing Company Ltd, Amsterdam, London, New York, 1970
2. John William Strutt, Baron Rayleigh, The theory of sound, Macmillan and Company Ltd, London,and New York, 1986
3. Douglas C. Giancoli, Physics Principles with Applications, Prentice Hall International Inc, 1991
4. Prof. Bell, EEE 450C notes, Dept of Electrical Engineering, UCT,1997
5. A.C Merrington, Viscometry, Jarrold and Sons Ltd, Norwich, 1949
6. J.R Van Wazer, J.W Lyons, K.Y Kim, R.E Colwell, Viscosity and flow measurements, Interscience Publishers, 1963
7. Mohan, Undeland, Robbins, Power Electronics, John Wiley and Sons, 1995
8. D.P Shaw, Automating the Control of a Research Experiment, BSc (Eng) Thesis, University of Cape Town, 1983
9. J.A Muaddi, Vibrational Methods Applied to NDT Testing and Fluid Density Measurement, PHd thesis, University of Aston in Birmingham, 1982
10. Y.A Rachman, Assessing Vibrating Viscometers in Slurries, MSc(Eng) thesis, University of Cape Town, 1977
11. C.J Smithells, Metals Reference Book, London Butterworths, 1962
12. Goran Stemme, Resonant Silicon Sensors, Departement of Solid State Electronics, Chalmers University of Technology, S-41296 Gotenborg, Sweden, 1990
13. Michel Christen, Air and Gas damping of Quartz Tuning forks, Sensors and Actuators, 1983
14. J.L.G Correia da Mata, J.MN.A Fareleira, C.M.B.P Oliveira, Cento de Quimica Estrutural, Departamento de Engenharia Quimica, Instituto Superior Tecnico, 1049-001 Lisboa, Portugal: http://www.zae-bayern.de/ectp/abstracts/correia da matal.html

15. Density simplified, General Science Archive
http://newton.dep.anl..gov/askasci/gen99/gen99428.htm
16. Hatschek Emile, The viscosity of liquids, G Bell and Sons Ltd, London, 1922
17. T.Lange, Measurement of viscosity using the tuning fork, Council for Mineral Technology, Measurement and Control Division, 1984
18. Density and Viscosity, Central Chemical Consulting
http://chem.com.au/newsite/dv.htm
19. Liquid Density Transducer
http://www.solartron.com/tranny/liqdensity.htm
20. Eexd, Haz Area Vibracon, Vibration Fork, Available:
http://za.rs.-c.dk/servlet/dk.stibo.module
21. Savant, Roden, Carpenter, Electronic Design Cicuits and Systems, Benjamin/Cummings Publishing Company Inc, 1991
22. G.Jack, Digital Electronics and Microprocessors (EEE 350W notes), Departement of Electrical Engineering, 1997

APPENDICES

APPENDIX A:

DATA OF VARIOUS TRANSDUCERS USED IN DIFFERENT LIQUIDS

APPENDIX B:

SOLATRON TRANSDUCERS

APPENDIX C:

TRANSDUCERS USED IN THE THICK LIQUID MEASUREMENTS

APPENDIX A:

DATA OF VARIOUS TRANSDUCERS USED IN DIFFERENT LIQUIDS

APPENDIX A

DATA OBTAINED FROM THE DECREMENTS OF THE VARIOUS TRANSDUCERS IN DIFFRERENT LIQUIDS

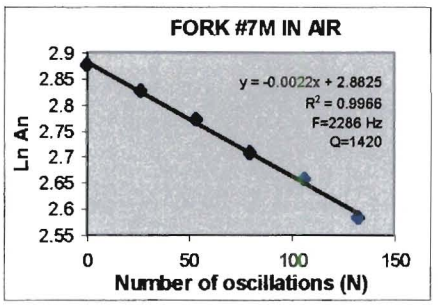

N	Ln An
0	2.876
26.5	2.826
53.1	2.773
79.6	2.708
106.1	2.657
132.6	2.584

Figure A.1: Results of a decrement obtained with a modified fork #7 (fork #7M) in air.

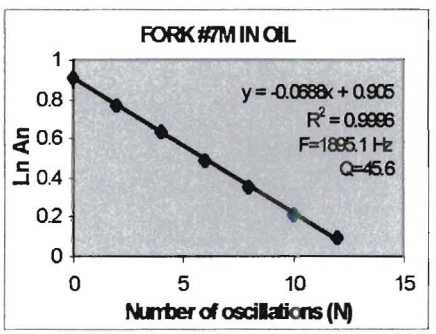

Ln An	N
0	0.91
2	0.768
4	0.629
6	0.486
8	0.352
10	0.21
12	0.09

Figure A.2: Results of a decrement obtained with a modified fork #7 (fork #7M) in oil.

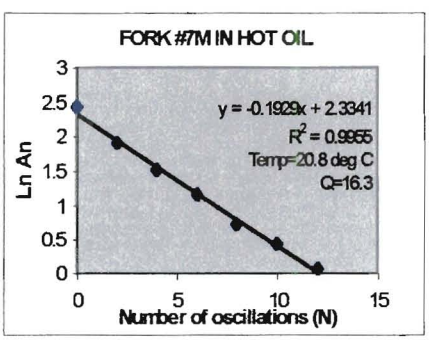

N	Ln An
0	2.42
2	1.91
4	1.518
6	1.159
8	0.724
10	0.446
12	0.06

Figure A.3: Results of a decrement obtained with fork #6 in oil.

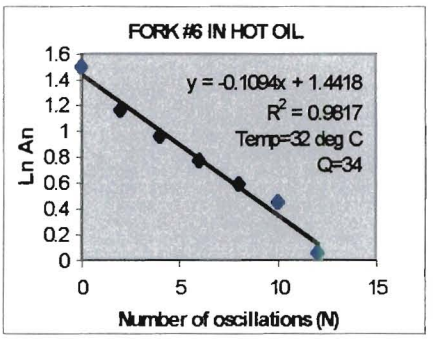

N	Ln An
0	1.504
2	1.159
4	0.965
6	0.768
8	0.594
10	0.446
12	0.06

Figure A.4: Results of a decrement obtained with fork #6 in hot oil.

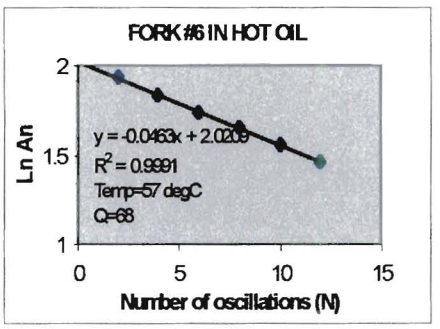

N	Ln An
0	2.015
2	1.937
4	1.833
6	1.738
8	1.658
10	1.558
12	1.461

Figure A.5: Results of a decrement obtained with fork #6 in hot oil.

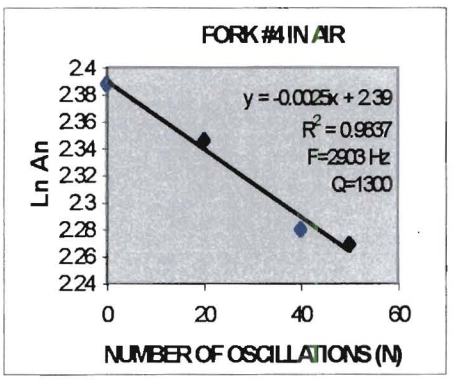

N	Ln An
0	2.388
20	2.346
40	2.28
50	2.269

Figure A.6: Results of a decrement obtained with fork #4 in air.

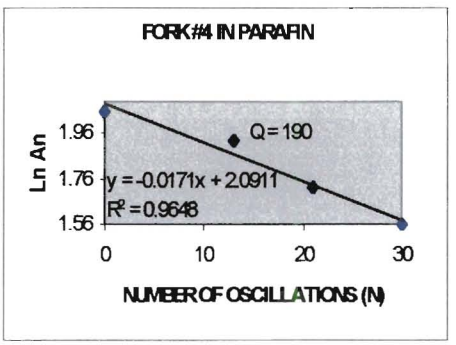

N	Ln An
0	2.06
13	1.93
21	1.72
30	1.56

Figure A.7: Results of a decrement obtained with fork #4 paraffin.

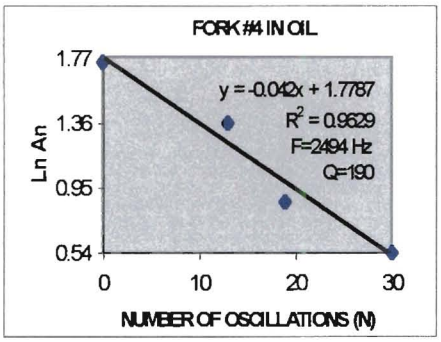

N	Ln An
0	1.75
13	1.361
19	0.862
30	0.54

Figure A.8: Results of a decrement obtained with fork #4 in oil.

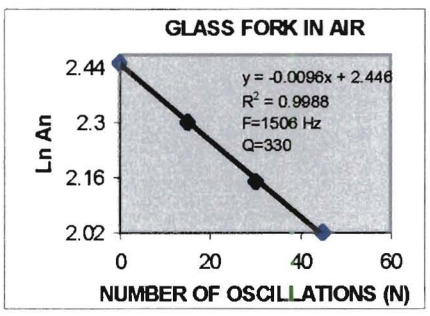

N	Ln An
0	2.45
15	2.3
30	2.15
45	2.02

Figure A.9: Results of a decrement obtained with a glass fork in air.

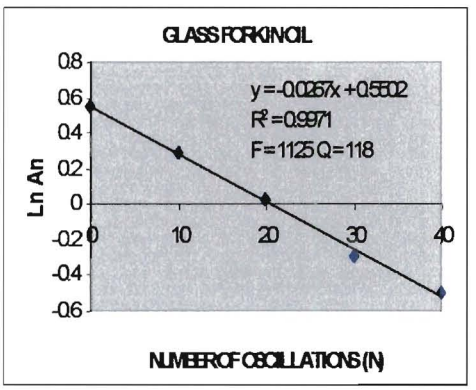

N	Ln An
0	0.554
10	0.285
20	0.025
30	-0.288
40	-0.494

Figure A.10: Results of a decrement obtained with a glass fork in oil.

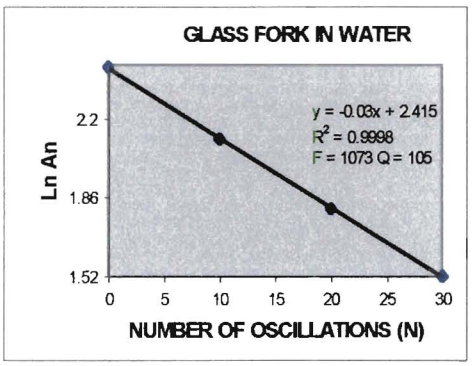

N	Ln An
0	2.42
10	2.11
20	1.81
30	1.52

Figure A.11: Results of a decrement obtained with a glass fork in water.

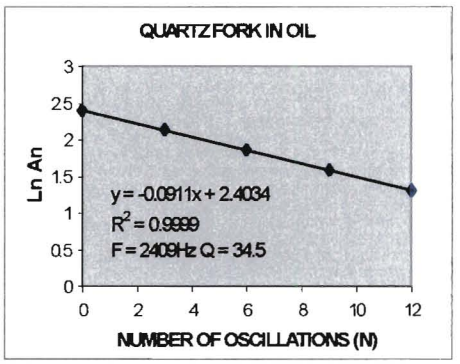

N	Ln An
0	2.398
3	2.133
6	1.863
9	1.585
12	1.306

Figure A.12: Results of a decrement obtained with fork #6 in oil.

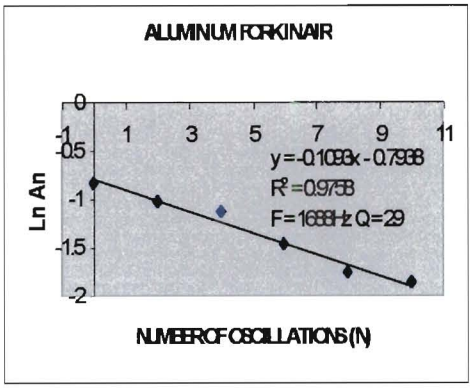

N	Ln An
0	-0.826
2	-1.024
4	-1.124
6	-1.465
8	-1.75
10	-1.852

Figure A.13: Results of a decrement obtained with fork #3 in air.

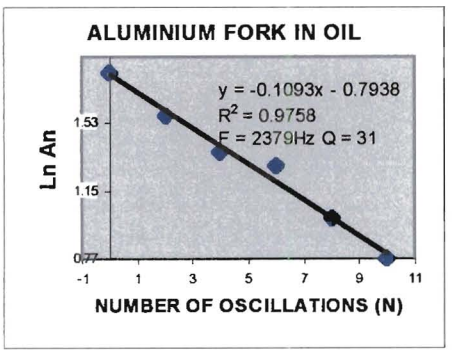

N	Ln An
0	1.812
2	1.571
4	1.364
6	1.287
8	0.997
10	0.77

Figure A.14: Results of a decrement obtained with fork #3 in oil.

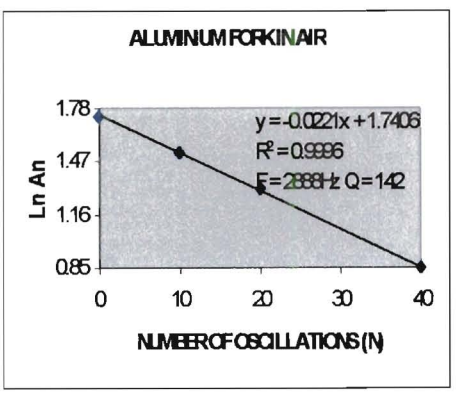

N	Ln An
0	1.733
10	1.524
20	1.306
40	0.85

Figure A.15: Results of a decrement obtained with fork #3 in air.

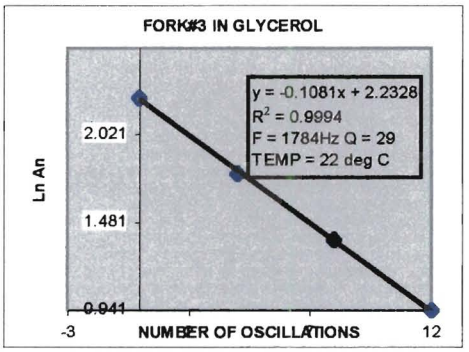

Ln An	N
0	2.245
4	1.781
8	1.371
12	0.941

Figure A.16: Results of a decrement obtained with fork #3 in glycerol at 22 deg C.

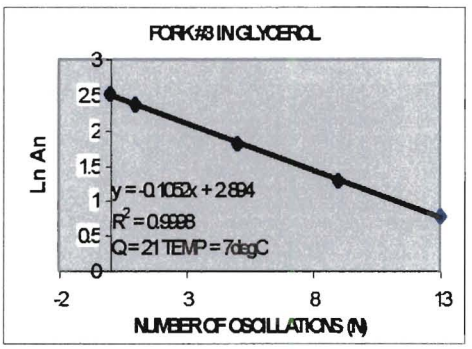

Ln An	N
0	2.51
1	2.369
5	1.812
9	1.289
13	0.783

Figure A.17: Results of a decrement obtained with fork #3 in glycerol at deg C.

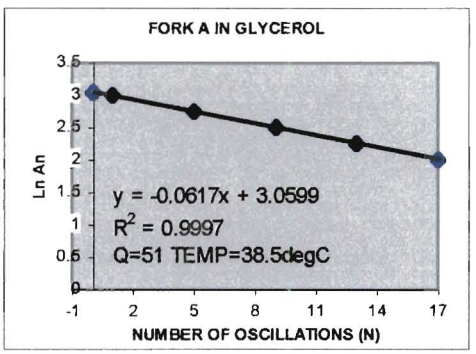

N	Ln An
0	3.047
1	3.005
5	2.757
9	2.51
13	2.258
17	2.006

Figure A.18: Results of a decrement obtained with fork #3 in glycerol at 38.5 deg C.

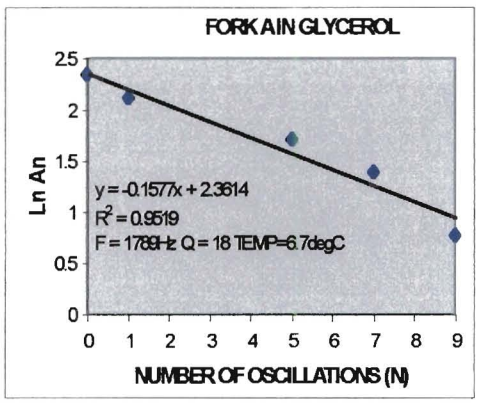

N	Ln An
0	2.34
1	2.125
5	1.71
7	1.394
9	0.768

Figure A.19: Results of a decrement obtained with fork #3 in glycerol at 6.7 deg C

APPENDIX B:

SOLATRON TRANSDUCERS

Solarton Transducers

Viscosity Measurement

Solartron's commitment to its customers to continually develop a range of high quality and reliable process instruments has resulted in the introduction of the Solartron process viscometer.

Using proven vibrating sensor technology the 7827 viscometer provides on line, continuous measurement of viscosity. Simultaneous measurement of density and temperature gives the instrument its unique advantage, permitting the accurate determination of dynamic and kinematic viscosity, which can be referred to standard conditions if required.

The system comprises of a sensor and conditioning electronics. The sensor can be simply installed in a by-pass, pipeline or tank. A choice of materials of construction and flange connections allows the sensor to be used in a broad range of process, liquids and pressures.

Independent calibrated ranges are available ensuring that the maximum accuracy is achieved. For applications where the measurement extends over more than one calibrated range an auto ranging facility in the conditioning electronics is provided.

Key Applications The 7827 process viscometer is ideally suited for:

- **Oil blending.** There is a need to determine the viscosity of an oil at standard conditions. This ensures the quality of the product which leads to efficient plant operation.
- **General process/Chemical** e.g. Glycol, clays, inks, fabric softener, resins, cement, shampoos, glue, detergents, varnish.
- **Pipeline interface detection.** The dual measurement of viscosity and density makes the Solartron process viscometer an ideal sensor for interface detection.
- **Pipeline leak detection.** One method in which leaks can be detected on major pipelines is by measuring the pressure drop over a given section of pipe. The pressure drop is a function of the on-line viscosity and density.

Principle of Operation
The 7827 operates on a vibrating element principle and can be regarded as a simple tuning fork maintained in resonance.

The damping of the vibration of the tines is proportional to the fluid viscosity. To be more exact the viscosity is inversely proportional to the square of the quality factor (defined as the resonant frequency divided by the band-width). The density of the fluid is determined by measuring the resonant frequency.

Liquid Density Measurement

The Solartron field proven range of densitometers have been designed to meet the most demanding

applications found in modern processing plants. These meters have long been recognized as the **Industry Standard.**

Where the high accuracy of the 7835 series is not required the 7826 Insertion densitometer provides the ideal solution. This unit can be mounted either in a static tank or in a pipeline.

All Solartron densitometers are available with a choice of flange and material of construction. This allows them to be used in a broad range of process liquids ensuring that Solartron has the answer to your metering and control requirements.

Fiscal Metering.
The **7835** is designed for fiscal metering of crude and refined hydrocarbons and non corrosive process liquids. This transducer offers the highest accuracy with excellent repeatability under pipeline operating conditions. The vibrating element is manufactured from Ni-Span-C for excellent long term and temperature stability.

General Process
Suitable for most general process applications, the **7845** is manufactured with all wetted parts in AISI 316L stainless steel. Typical applications are:

- Percentage mass, percentage volume and specific gravity of fluids or fluid/fluid fluid/solid mixes.
- Caustic soda blending. Concentrated product delivered by road tanker is diluted with water for on-site storage.
- Energy conservation in whisky distilling. Used to monitor the alcohol content and shut off the heat source when the value of the alcohol falls to near the cost of the energy consumed.
- In the sugar industry for controlling degrees Brix.
- Interface detection
- Blending control

Corrosive Applications
For corrosive applications where AISI 316L stainless steal is not suitable, the **7846** offers wetted parts in Hastelloy C22.

Hygienic Applications
Solartron densitometers are widely used in the food industry for the monitoring and control of foodstuffs, for example, milk and yogurt. The 3A- authorized, all stainless steel **7847** with special bellows make it an ideal solution. Various sanitary fittings are available for the transducer.

Insertion Densitometer
The **7826** Insertion Densitometer has been developed for applications requiring liquid density measurement in pipelines or static tanks.

The **7826** consists of a tuning fork arrangement with the tines mounted from a flange, which in turn supports the electronics housing. The transducer is available in a range of flange options, including a 3A authorized unit. An integral 4-20mA version is available.

Principles of Operation
All Solartron liquid density transducers operate on the same general principle and can be likened to

that of spring mass system. As the product density changes it in turn changes the vibrating mass, which is then detected by a change in the resonant frequency.

When a mass on a sperm is displaced and released it will oscillate at a natural frequency until it comes to rest due to viscous damping. An oscillation at the natural frequency may be maintained by supplying a driving force to overcome the effects of damping.

Solartron Transducers
11321 Richmond Ave. M-102
Houston, Texas 77082-2615
USA
Tel: 1(713) 558-2587
Fax: 1(713) 558-8954

Liquid Density Transducers

Based on Solartron's vibrating element technology, the **7835/45** family of Liquid Density Transducers are well established as the industry standard for on-line applications, feature a unique single straight-tube design. The **7826** transducer can be inserted into a tank or pipeline. Both types - which use a measurement technique based on a vibrating element - can handle liquids and slurries, and provide continuous, accurate instantaneous measurements.

The new 7828 digital insertion density transmitter offers a direct 4-20mA output of line or base density, or other selectable density-based values.

- Straight-through flow path reduces pressure drop, minimizes maintenance
- No moving parts or seals
- Unaffected by vibration
- Insensitive to flow and pressure variations
- Wide range of materials available to suit most applications
- Approved for use in hazardous areas
- Entrained Gas version available

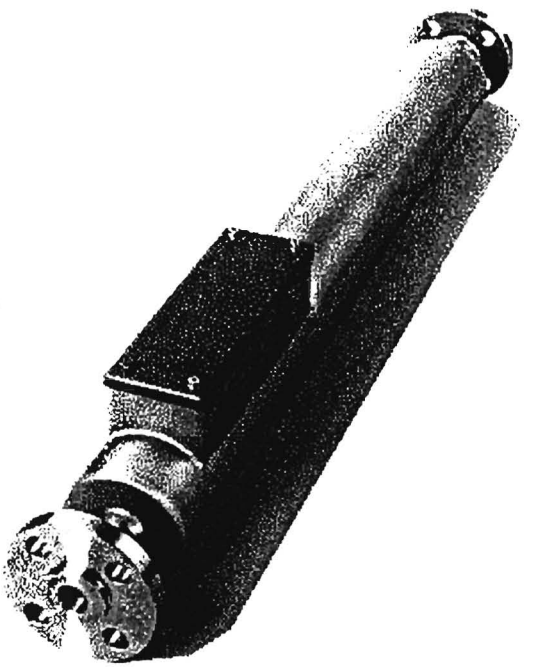

Typical applications

- Fiscal metering
- Slurries
- Food processing
- General chemicals
- Hydrocarbons
- Resource management

Typical measurements

- API degrees
- Degrees Twadell
- Absolute and Referred Density
- Concentration by mass or volume

Advanced Density System

Solartron has significantly expanded the application of liquid density measurement by integrating

signal processing into the 7835 Family of Density Transducers.

- Lower cost installation
- Industry standard communication
- Direct analog and digital outputs
- Remote display option for local analysis or set-up
- Modular upgrade and expansion

Solartron's vibrating element technology

The majority of Solartron's transducers are based on the vibrating element principle: the element is electromagnetically excited at its natural resonant frequency, which is dependent on the density of the fluid or gas surrounding the element. The resonant frequency is maintained electrically, and any change is detected and used to derive the change in density of the surrounding fluid or gas. (Viscosity can also be derived by measuring the "Q-factor" from the half-power (3dB) frequencies either side of the resonant frequency.)

Return to Industrial Products main page...

APPENDIX C:

TRANSDUCERS USED IN THE THICK LIQUID MEASUREMENTS

APPENDIX C:

TRANSDUCERS USED IN THE THICK LIQUID MEASUREMENTS.

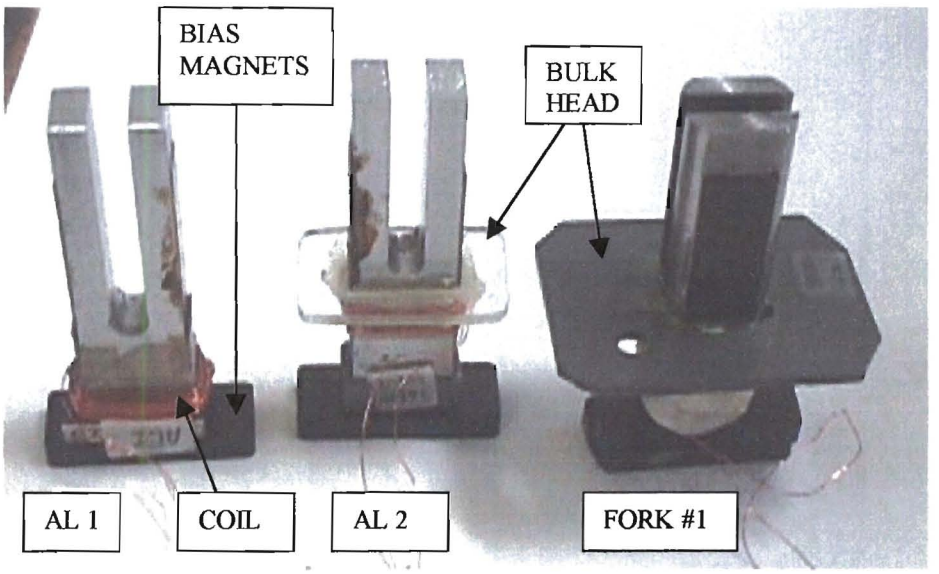

Figure C.1: These transducers are the best ones developed for liquid measurements.

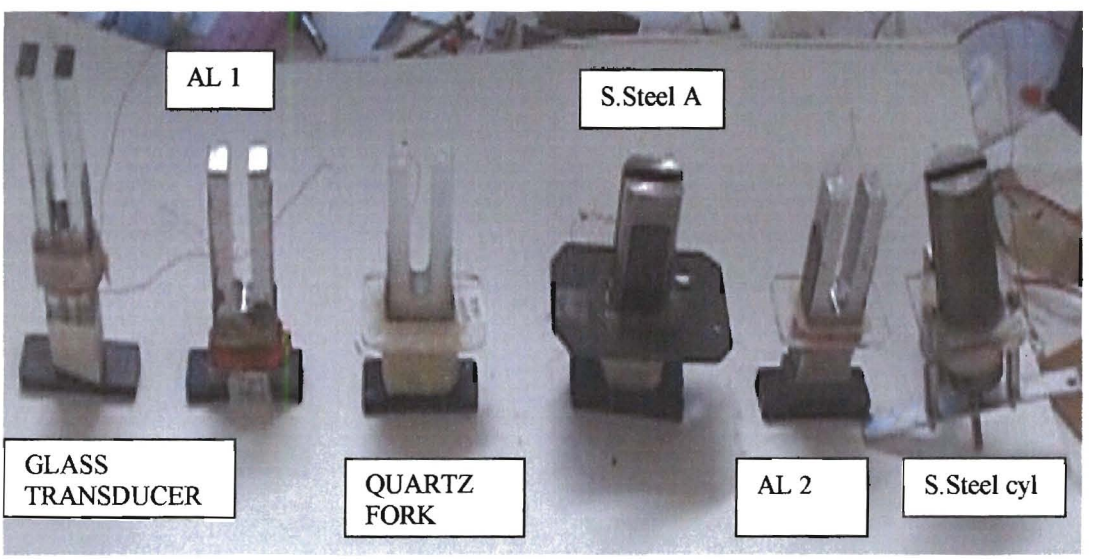

Figure C.2: The improved transducers used for the characterisation of liquids.